FROM ART TO PART:

A SIMULTANEOUS GEOMETRY AND DECORATION WORKFLOW

By

YAJIE JIANG, B.A.Sc.

A Thesis

Submitted to the School of Graduate Studies

In Partial Fulfillment of the Requirements

For the Degree

Masters of Applied Science

McMaster University

Masters of Applied Science
(Mechanical Engineering)

McMaster University
Hamilton, Ontario

TITLE: From art to part: A simultaneous geometry and decoration workflow.

AUTHOR: Yajie Jiang

SUPERVISOR: Dr. Allan D. Spence

NUMBER OF PAGES: ix, 87

Abstract

Reproduction of hand crafted 3D shape geometry is an important industrial concept design step employed for items ranging in size and function. Adding surface art work can extend concept design to include essential product information.

This thesis describes an equipment and workflow implementation for reproducing both 3D shape and art work. The hand crafted sample shape is laser digitized to obtain the XYZ geometry coordinates simultaneously with the surface gray level. The resulting point cloud is processed and converted to an STL format for plastic rapid prototyping, while the surface gray level information is treated to fit the smoothed surface, and match the reproduction ink jet printing system resolution and specification. Developed software automatically calculates the dot pattern to reproduce the art work onto the correct prototyped surface location.

Acknowledgments

This thesis arose in part out of years of research and work that has been done since I came to Dr. Spence's group. This research project would not have been possible without the support of many people. It is a pleasure to deliver my gratitude and appreciation to them in my humble acknowledgment.

In the first place, I would like to express the most truthful gratitude to Dr. Allan D. Spence for his invaluable guidance, encouragement, infinite patience and financial support. His truly scientist-engineering and educating intuition has made him as an honorable and knowledgeable professor, who inspires and enriches my experience of growth as a student and researcher.

To Dr. Spence's research group members, especially, Simon El Sahi, I would like to thank them for their friendship, meaningful help and suggestion for my research and work.

Finally, I feel grateful to have enormous support and motivation from my family. My wife, Shan, delivered a lovely baby boy this year. My parents not only financially supported my life but also took good care of my wife during her pregnancy. To my wife, she has taken major responsibility for the baby to allow me focus on my study since then. It is beyond any words to express my love to them.

Nomenclature

CAD – Computer Aided Design

CMM – Coordinate Measuring Machine

RGB – Red Green Blue

FEA – Finite Element Analysis

RP – Rapid Prototyping

FDM – Fused Deposition Modeling

ABS – Acrylonitrile Butadiene Styrene

PTP – Pad Transfer Printing

CVs – Control Vertices

PCD – Point Cloud Data

B-Rep – Boundary Representation

CSG – Constructive Solid Geometry

DPI – Dot Per Inch

FOV – Field of View

TTL – Transistor Transistor Logic

P_s – Simplified Point Cloud Data Cell Array

I_{gray} – Gray Scale Intensity Matrix

MCS – Machine Coordinate System

PCS – Part Coordinate System

M_p – Transformation Matrix from PCS to MCS

Table of Contents

List of Figures

Chapter 1
Introduction

A study of recent manufacturing industry shows the high percentage of product failure is attributed to design inadequacies. In order to reduce the quality cost, more and more companies are pushing quality improvement actions to focus on product design and development stage [1]. However, product design and prototyping usually require many modifications, reruns, and reproductions of concept models.

In the current market place, 3D Art to Part is a popular applicable process to reproduce any design concept, such as 3D hand crafted artistic shapes. This process can be regarded as an individual stage for new product development to optimize and facilitate volume production [2]. By implementing 3D art to part technologies, integration of product development can be achieved through easy interfacing of product design with consideration of product viability, including product test, verification and validation. Most commonly, 3D art to part includes applications of technologies such as laser digitizing, rapid prototyping and applications of corresponding CAD tools. In the fields of fine arts and archaeology, there is interest in additionally reproducing item surface coloring. Such ability would permit public display of the reproductions, while fragile originals are safely stored [3, 48].

Prior development of the oriented inkjet printing solution is described in the master thesis by El Sahi [48]. The current thesis extends the implementation to include laser digitizing and advanced B-Spline surface modelling. The full workflow, therefore, utilizes laser digitizing, rapid prototyping, applications of CAD tools and 3-

D ink-jet printing. To fulfill integration of the product development workflow, a CMM-laser digitizing system and a oriented 3-D printing system [3] are realized by mounting laser digitizer and ink-jet printer with rotating probe head onto two Coordinate Measuring Machines (CMM).

An actual sample produced by the workflow is illustrated using aesthetic shape. The workflow is repeatable and easy to implement. The knowledge of this workflow implementation and process setup provide meaningful help to those customers who specialize in new product design and development.

The remainder of the thesis is organized as follows. Chapter 2 contains the literature review that explains all technologies involving in the project. Chapter 3 describes the equipment setup for employed CMM-laser digitizing system and oriented 3-D printing system, as well as their specifications. Chapter 4 discusses the details of the introduced workflow implementation. The corresponding sample experiment results for each process of the workflow are displayed in chapter 5. Finally, chapter 6 concludes the thesis.

Chapter 2
Literature Review

The 3D art to part concept, as a bringing-art-ideas-to-life process, is more widely applied in manufacturing, allowing the design engineer to create a linkage between product artistic aspects and product engineering specification. The equipment used by 3D art to part are extremely versatile but the major workflow are common [4]. The accomplishment of a typical geometric art-to-part process is based on technology applications of laser digitizing, rapid prototyping, and corresponding applied CAD tools with attentions to related theories and algorithms. Reverse engineering work for product decoration applies technology of 3D printing from 2D images. In this chapter, all these fields of technologies will be reviewed.

2.1 Laser Digitization

3D laser digitization is a technology developed to digitally capture geometric shape of physical objects. Laser triangulation is common technique for laser digitization, where the distance of the object is computed by means of a directed laser source and a light sensitive receiver array [5]. The employed Hyscan 45C/SC2 laser digitizer [6], based on the principle of triangulation, computes 3D coordinates using a synchronized scanning scheme [7] (see figure 2.1 and 2.2).
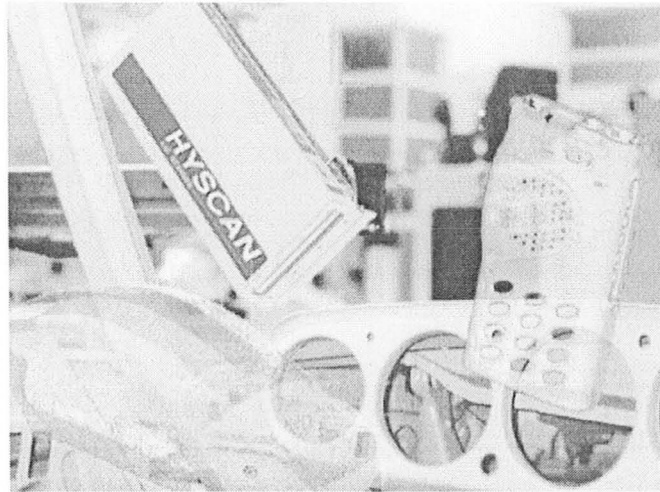
Figure 2.1 Hymarc Digitizing Camera [6]
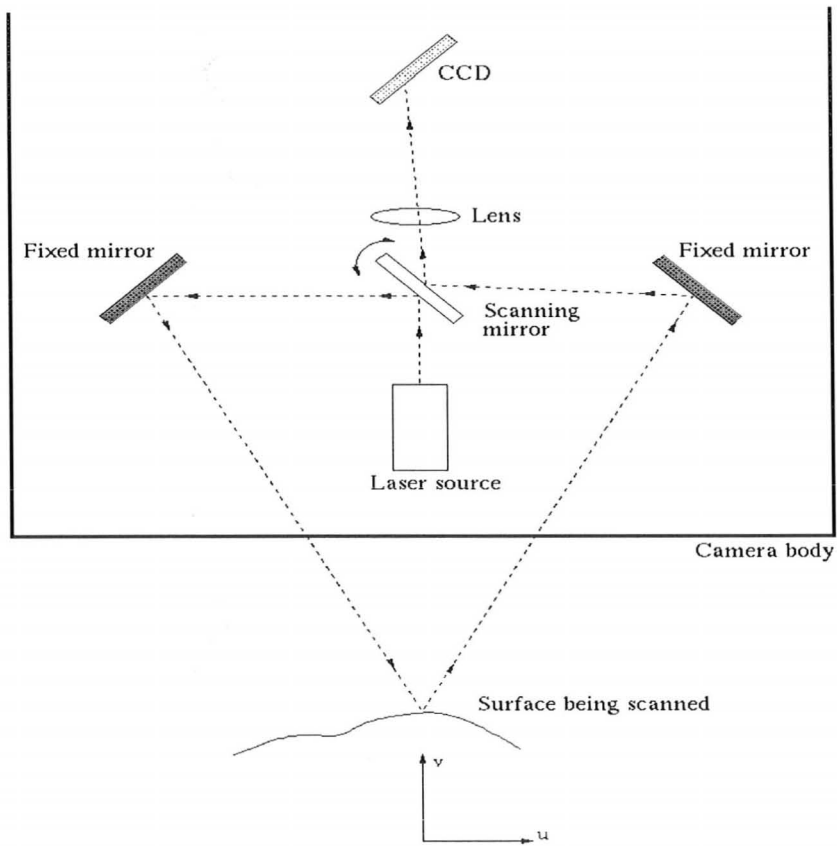
Figure 2.2 Principle of Laser Digitizing [7]

The body camera of the Hymarc digitizer contains a Charge Coupled Device array, (CCD array) two fixed mirrors, lens, oscillating mirror and laser diode. The CCD array is a digital camera that includes large number of photosensitive elements. In figure 2.2, laser beam is projected onto a double-sided scanning mirror that provides synchronization between projection and detection. The projected beam is directed by the scanning mirror onto the scene, and reflects off the surface of the scanned object. The returned beam is directed by back side of the oscillating mirror, and received by a linear positioned charge coupled device array (CCD array). Then, the system determines the (U, V) and oriented scanning mirror angle θ for calculation of captured position with its peak intensity I from CCD camera. To calculate intensity information I, each photosensitive element of CCD generates electrical charge that is proportional to light intensity, so that each recorded intensity value for a certain position relates to a correspondent charge coupled element.

There are essentially three main types of 3D laser digitizers: handheld digitizers, tripod based digitizers [8] and CMM based digitizers. Handheld digitizers are portable and able to scan objects in their natural environment with relatively fast data collection and low accuracy, such as the currently developed handy digitizers by Creaform [9] (see figure 2.3 a)). Tripod based digitizers restrict digitized objects and environments to be constructed within certain range of angles and distances. The scanning and sweeping movements are controlled and constrained from the environment conditions; such as FARO's quantum arm digitizer [10] displayed in figure 2.3 b). A CMM based digitizer, such as Metris CMM laser scanning system [11] shown in figure 2.4 c), allows motion of digitizer to be controlled by CMM, where the stability and accuracy can be highly ensured. The employed CMM-Hymarc laser digitizing system in this thesis is also a typical example for CMM based digitizer.

The development of laser digitizing technology continuously improves in the fields of scanning scale and accuracy with higher definition performance. For instance, the recent developed FARO Photon is able to capture a 25 m ranged building geometry with measuring error less than 2 mm [10]. The primary performance criterion for industrial laser digitizing systems is a trade-off between measuring accuracy and measuring range [12, 13]. The measuring range extends of points from

some centimeters to hundreds of meters, and scanning speed from hundreds per second to hundreds of thousands of points per second. The achieved accuracy ranges from less than 20 μm to centimeters depending upon the working volume.
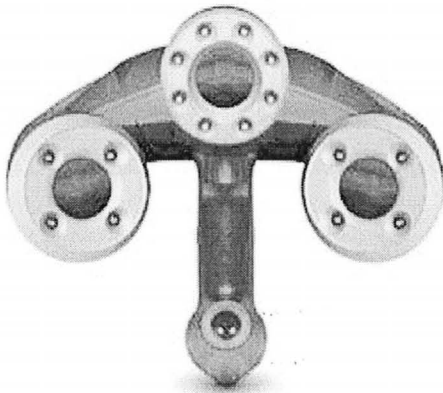
a) Agile's Handy Digitizer [9]   b) FARO Quantum Arm Digitizer [10]
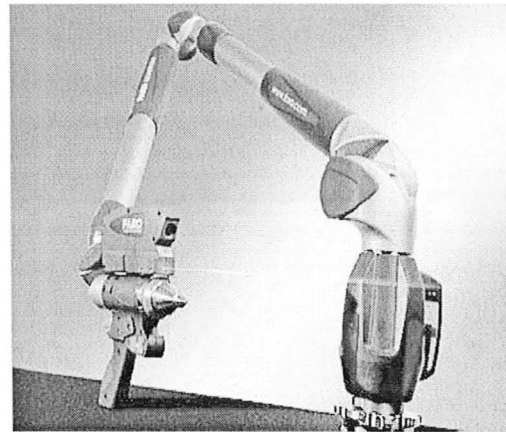
c) Metris CMM Based Digitizer [11]

Figure 2.3 Examples of Laser Digitizers

Taking accuracy, sampling density and uniformity into consideration, connecting digitizer to CMM guarantees a balance between data quality and life time cost through CMM capability of orthogonally moving its end-effector in a rectangular volume with very high precision [12]. Extension technology of simultaneous capturing image color RGB [14], or intensity gray levels, not only provides the application of 3D image visualization but also allows the implementation of accurate determination and analysis of product mechanical properties, such as high accurate sheet metal strain and surface analysis [15].

The most typical industrial fields of applications for laser digitization include military, aerospace, automotive, light and heavy-duty manufacturing, consumer production, medication, art and architecture etc. For example, the most well-known application for automotive industry is vehicle body styling [16]. From figure 2.4, a 3D laser digitizer accurately captures the fine details and curves of the body panels', and eliminates costly prototypes by starting with good data. By CAD modeling, re-engineered body part is designed, where reworking and fabrication time are sufficiently reduced. This engineering reverse work of good quality CAD modeling also provides an easy accessibility for performance verification and Finite Element Analysis (FEA).
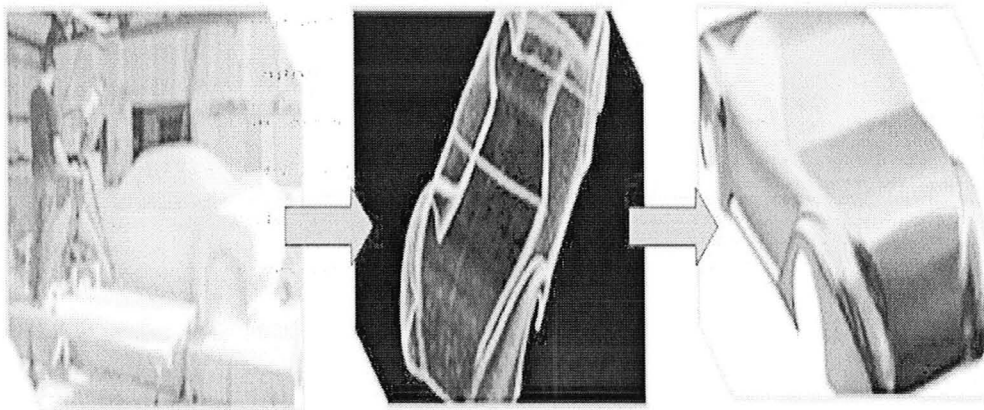
Figure 2.4 Digitizing Sample Application [16]

2.2 Rapid Prototyping

Rapid prototyping (RP) is an additive manufacturing process that can directly construct a product from CAD designed digital model [17]. The history of this technology development is closely matched with the development of CAD and CAM traced from manual prototype, virtual prototype to rapid prototype [18]. The process allows free concept design without usual manufacturing constraints. The intention of this technology is to physically realize the conceptualization of design using the CAD

data file.

In product design and development, prototyping plays a very important role. It is used to help planning, experimenting, testing, and verifying the product ideas and specifications [18]. The convenience of rapid prototyping process allows iterative building of the prototypes during the product design and development stage; so that the actions of product design debugging and root cause analysis are easy to iteratively deploy [19]. Iteration of prototyping for product concept development guarantees better product competitive power through achieving a higher percentage of product conformity and customer satisfaction [18].

From the most accepted method in market, RP systems can be classified into three types: liquid-based, solid-based and powder-based. The classification is based on initial forms of their loaded materials [18]. In liquid-based system, where initial material converting from liquid to solid during the process, rapid prototyping is possible under the "photo-curing" method [20, 21]. This single laser beam method is the most commonly applied method to simultaneously allocate prototype constructing position in the processing environment. Solid-based 3D RP systems, however, employ solid forms of materials, such as, rolls, laminates and pellets. It is referred as "Cutting and Gluing" method [18] for half-solidified melt-down materials. Also, powder-based systems apply same prototype constructing method as solid-based systems with initial material of grain-like form.

In the thesis project, the employed Dimension BST Printer [22] shown in figure 2.5 is a solid-based RP machine with major commercial application technology of Fused Deposition Modeling (FDM) that is explained in figure 2.6. Stratasys' FDM, initially developed in 1991 [22, 23], is a commonly used technology in rapid prototype machines. Basically, the solid material, for example Acrylonitrile-Butadiene Styrene (ABS) or other thermoplastic polymer, is settled as coiled filament in the cartridge. When operating the RP system, the filament is fed to the extrusion heat chamber. The plastic material is pre-heated to the temperature just below solidification point. The extrusion nozzle applies the semi-liquid filament on to the x-y plane platform. The quickly solidified filament forms a very thin layer, which can be regarded as realization of 2D cross section for the CAD model at the specific level along z axis. For instance, the employed Dimension BST Printer in this thesis has a

resolution of 0.01". With steps of descending the platform along z-axis, the extrusion nozzle glues the each 2D layer onto its previous one to form the prototype. The extrusion nozzle ends each step of layer building with cutting process of the feeding filament.
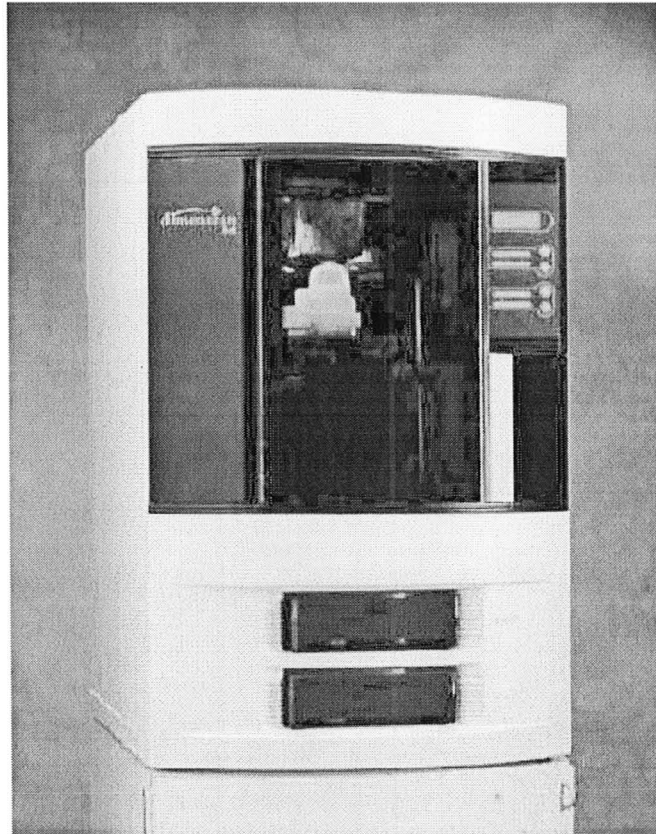
Figure 2.5 Employed Dimension BST RP Printer [22]

2.3 Prototype Decoration with 3D Printing

According to Hillestad et al. [24], it is better to consider product decoration during the design process, where decoration is defined as the application of a finish or graphic that adds value to the final product. Therefore, adding the decoration to the iterative prototypes can help designer to achieve better quality results. The decoration

process is usually a printing process to deposit 2D patterns to 3D surfaces. The most common technology is Pad Transfer Printing (PTP), where an automatic stamping process is applied [25]. However, all currently applied decoration printing processes share the same demerit of high initial cost and poor suitability for low quantity prototyping.
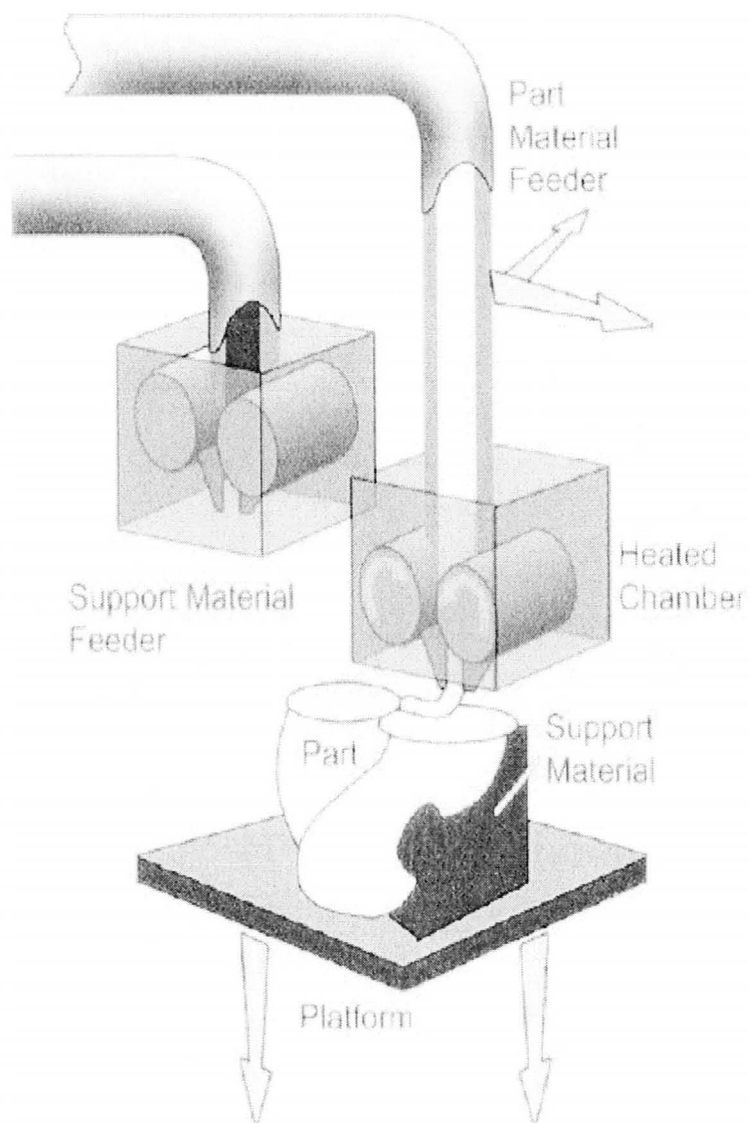
Figure 2.6 FDM System Schematic Drawing [23]

2.4 Usage of CAD Tools

2.4.1 Coordination of CAD Tools

Imageware [26], Autodesk Inventor [27] and AliasStudio [28] are employed in this thesis to separate the CAD model establishment into conceptual and detailed stages. From proper sequential usage of different CAD tools, debugging of product design can be addressed to the conceptual stage regardless of process history, so that time cost for product development is greatly narrowed.

CAD Surface Modeler

AliasStudio [27] is one of the most powerful CAD software package for forming and editing complex smooth surfaces. In AliasStudio, any surfaces, constructed by curves, can be controlled and represented by their hull, where lines between consecutive control vertices (CVs) form the control hull. By editing the control vertices on the hull, we are able to shape up the surface. Lines of the hull give the parametric U and V directions. This allows us to create and edit any kind of smooth surfaces as figure 2.7 depicted. In addition, with trimming and stitching tools, it is capable to generate any sculptured surface. However, it is only the surface that can be generated by this CAD software.

CAD Solid Modeler

To thicken a surface and add detailed design, it is necessary to build CAD solid model from other functional CAD tools, such as Inventor [28]. Since any surface editing any modifying are addressed by surface modeler solid modeler is only used to convert the imported general surface model to thickened solid model, as well as design of detailed features.
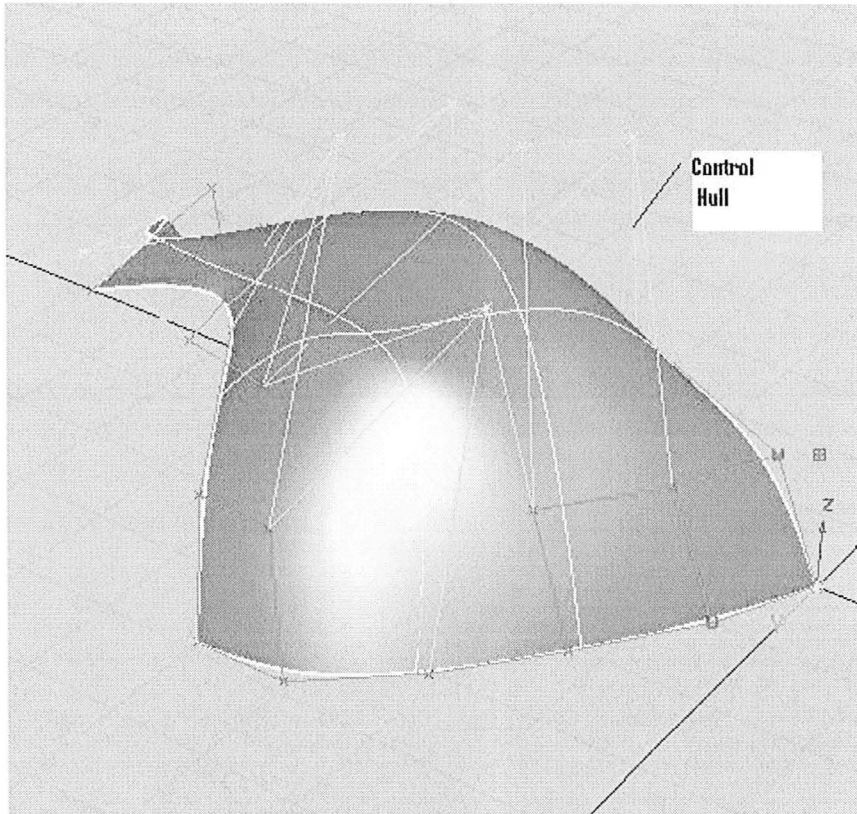
Figure 2.7 Capability of Surface Modification for AliasStudio

CAD and PCD Verification Modeler

Imageware [26], used in this thesis, allows excellent interfaceability to digitized point cloud data (PCD), so that it can be accurately converted to final CAD surface model, as well as the easy operational CAD model verification to digital sape of original hand crafted model. This CAD tool provides unique and comprehensive approach to 3-D modeling with capabilities of advanced modeling, reverse engineering, CAD inspection and polygonal modeling [26]. From the software, quality design workflow is achievable with maximum control for checking model aesthetics, conceptual consistency, fidelity, and surface smoothness etc.

2.4.2 CAD Data Exchange

For any commercial CAD system, designed objects are saved as the system default files with two major structures: Constructive Solid Geometry (CSG), Boundary Representation (B-Rep) [29, 30]. They are also the most common topologies that are used in CAD systems. For example, the employed Inventor uses B-Rep topology to store the geometric data in a tree structure shown in figure 2.8. Although the types of default files can be quite versatile the concepts of data structures are generally belong to the two techniques. This allows data exchange translators [29] to be developed for exchange of modeling data in different CAD systems.
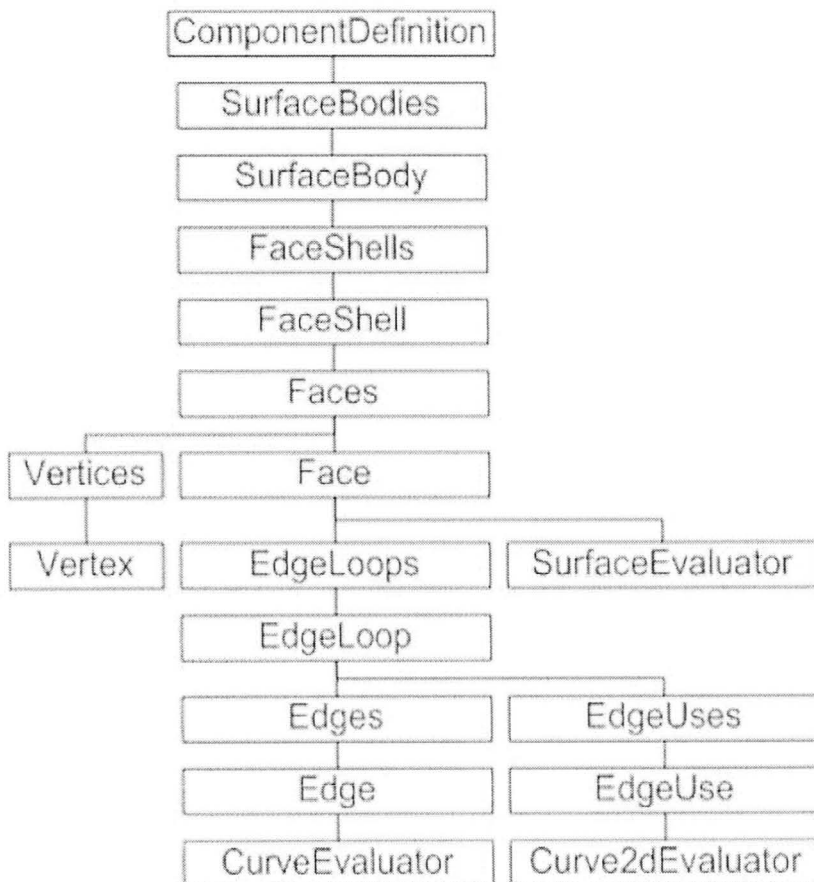
Figure 2.8 B-Rep Topology [28]

There are two solutions for data exchange translators: direct and indirect [29]. Shown in figure 2.9, direct translator converts the data format from native systems to the other in one step. Indirect translators are only available for the neutral formats files, such as IGES and STEP. For example, IGES is the first standard exchange format developed as neutral that supporting for both B-Rep and CSG scheme [29].

AliasStudio and Inventor, with built-in direct translators, are capable of reading default data files from each other in 2008 and later versions. However, this is not possible for Imageware. The solution of transferring PCD is to make a standard IGES file as neutral base.

Furthermore, STL has become a neutral CAD data format that is used in rapid prototyping industry. STL is a facet representation to approximate total object geometry with adjustable facet resolution [29, 31]. In STL file, each facet is built from a normal and three vertices, and two adjacent facets share two vertices with each other. Described in figure 2.10, CAD model is triangulated into small pieces to evaluate the real shape. By defining higher resolution of STL file, it is possible to produce a better quality RP model only if the RP machine allows.

(a) Direct translators   (b) Indirect translators
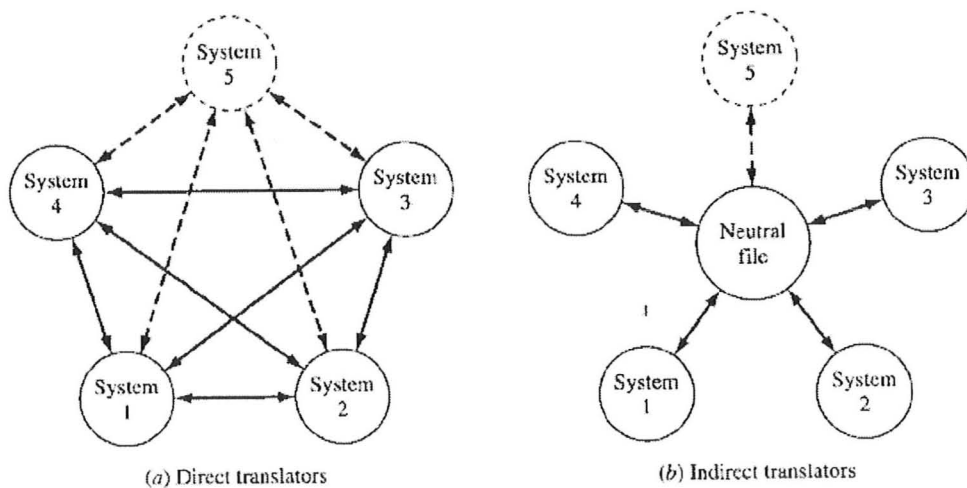
Figure 2.9 Types of CAD Data File Translators [29]

```
solid ascii
  facet normal -3.077349e-001 9.099792e-002 9.471107e-001
    outer loop
      vertex   -1.000000e+001 2.000000e+000 1.180000e+002
      vertex   -9.807882e+000 3.950339e+000 1.178750e+002
      vertex   -1.058779e+001 2.000000e+000 1.178090e+002
    endloop
  endfacet
  facet normal -3.728222e-001 1.179300e-001 9.203782e-001
    outer loop
      vertex   -1.058779e+001 2.000000e+000 1.178090e+002
      vertex   -9.807882e+000 3.950339e+000 1.178750e+002
      vertex   -1.043786e+001 4.382389e+000 1.175645e+002
    endloop
```
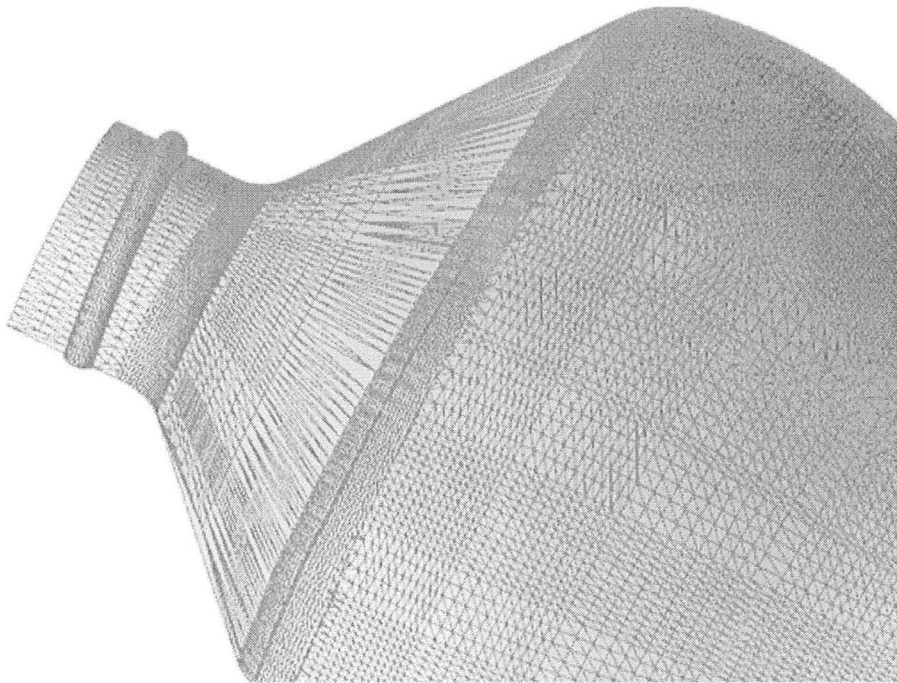
Figure 2.10 Sample of Triangulation of STL File

2.5 Required Fundamental Knowledge of CAD

The strategy for the approach of this thesis requires basic CAD knowledge of B-Spline curves and surfaces, Coons patch surfaces [29] and practical application of Uniform Parameterization B-Spline Least Squares Fitting algorithm [32, 33].

2.5.1 B-Spline

Curve

A B-Spline Curve is an effective mathematical way for CAD tools to define smooth curves from data points [29]. B-Splines allow curve design with different degrees of continuity according to engineering applications. Any section of a B-Spline can be defined by a certain number of control points with specific degree. For example, recent CAD tools usually offer a default B-Spline function box for design of cubic B-Spline curves, requiring four control points to represent each span of the curve. The mathematical expression of B-Spline curve, based upon uniform parameterization, contains three major parts, such as basis function N(u) in 2.2 and 2.3, control points P(x, y, z), and corresponding curve points Q(u) in function 2.1. The curve functions can be represented as the following:

$$Q(u) = \sum_{i=0}^{n} P_i N_{i,k}(u), \quad 0 \le u \le u_{max} \qquad (2.1) \,[29]$$

with the interpolation of basis function as:

$$N_{i,k}(u) = (u - u_i)\frac{N_{i,k-1}(u)}{u_{i+k-1} - u_i} + (u_{i+k} - u)\frac{N_{i+1,k-1}(u)}{u_{i+k} - u_{i+1}} \qquad (2.2)\,[29]$$

where

$$N_{i,1} = \begin{cases} 1, & u_i \le u \le u_{i+1} \\ 0, & otherwise \end{cases} \qquad (2.3)\,[29]$$

In the expressions, i is the control point number. The parameter k controls the continuity degree. The global knot parameter u locates in a certain range with respectful boundary condition u_i and u_{i+1}. The boundary condition is defined by its correspondent span of two adjacent data points on the curve. For any B-Spline curve span with cubic degree, the mathematical expression can be written as function 2.4:

$$Q(u_i) = P_i N_{i,4} + P_{i+1} N_{i+1,4} + P_{i+2} N_{i+2,4} + P_{i+3} N_{i+3,4} \qquad (2.4)\,[29]$$

B-Spline Surface and Coons patch Surface

A typical B-Spline surface, swept from curves, is constructed from a rectangular set of data control points, where the uniform parameters are two dimensional. The function of a typical B-Spline surface can be written as the formula 2.5 with $(n+1) \times (m+1)$ array of control points.

$$S(u,v) = \sum_{i=0}^{n} \sum_{j=0}^{m} P_{ij} N_{i,k}(u) N_{j,l}(v) \qquad (2.5)\ [29]$$

In this expression, $S(u,v)$ is any point on the surface, where k and l represents the surface order in u and v direction. The control points establish the vertices of characteristic polyhedron of the resulting surface [29].

Furthermore, Coons patch is used in blending four prescribed intersecting curves to form a square-like closed boundary [29]. The four boundary curves can be represents as $C(u, 0)$, $C(1, v)$, $C(u, 1)$ and $C(0, v)$, where all boundaries are identically parameterized in pairs. The parameters, u and v, range from 0 to 1. The function 2.6 is the expression of a Coons patch surface, where $C(u,v)$ is any corresponding surface point controlled by parameterized vertices.

$$C(u,v) = -\begin{bmatrix} -1 & (1-u) & u \end{bmatrix} \begin{bmatrix} 0 & C(u,0) & C(u,1) \\ C(0,v) & C(0,0) & C(0,1) \\ C(1,v) & C(1,0) & C(1,1) \end{bmatrix} \begin{bmatrix} -1 \\ 1-v \\ v \end{bmatrix} \qquad (2.6)\ [29]$$

AliasStudio offers the operational function box for Coons patch surface construction, named as 'square surface' [26], which is used in this thesis.

2.5.2 B-Spline Least Squares Fitting Algorithm

Application of a B-Spline fitting algorithm is a very useful method for smooth curves definition and simplification. A set of data, measured or scanned from a real object, can be simplified and reconstructed in CAD system, according to a defined tolerance, for design and inspection purposes.

The applied B-Spline fitting algorithm in this thesis is a uniform parametric least squares fitting algorithm, so that the uniformity comes through equally assigned sample points of the estimated B-Spline curve [32]. This is the major assumption of the algorithm. The detailed procedure for generating simplified cubic B-Spline curve is listed with the functions from 2.7 to 2.9 as following:

1. Define least squares error function as expression 2.7, where k represents the quantity of recorded sample data, and j represents the quantity of desired control points for simplified curve.

$$E = \frac{1}{2}\sum_{k} \left\| \sum_{j} N_{j,4}(u_k)P_j - Q_k \right\|^2 \qquad (2.7)\ [32, 33]$$

2. Least squares minimization can be achieved by zeroing the partial derivatives of the error with respect to control points.

$$\begin{aligned} \frac{\partial E}{\partial P_i} &= \sum_{k}(\sum_{j} N_{j,4}(u_k)P_j - Q_k)N_{i,d}(u_k) \\ &= A^T AP_j - A^T Q_k \qquad\qquad (2.8)\ [32, 33] \\ &= 0 \end{aligned}$$

where A is the matrix with total j rows.

3. After re-writing the formula, expression of simplified control points can be presented as matrix form of 2.9. The ill condition of the matrix inversion in function 2.9 due to the nearly zero eigenvalues can be solved from singular value decomposition [34].

$$P_j = (A^T A)^{-1} A^T Q_k \qquad (2.9)\ [32, 33]$$

4. Simplified B-Spline can be defined from the input of control points or the curve sample points calculated from control points.

2.6 Summary

In this chapter, all applied technologies have been reviewed with the importance emphasized for product development. The introduced technology included laser digitizing, rapid prototyping and corresponding CAD tools. In addition, the related basic CAD knowledge has been discussed as well as the theories and algorithm. The remainder of the thesis will illustrate the detailed workflow, where the approach of all these technologies and algorithm will be pointed out.

Chapter 3

Equipment Setup

This chapter illustrates two system architectures with detailed information and specifications of their major devices. The two systems were established to achieve different purposes in this thesis. A CMM-Hymarc laser digitizing system is used to fulfill the objective of product geometry and surface intensity digitizing. In order to accomplish image printing on the rapid prototype surface, an oriented 3-D ink-jet printing system [3] is used.

3.1 System Components

Both systems include major structures of coordinate measuring machines (CMM) with sub devices as Renishaw PH10 [36] probe head, touch trigger probe, serial ink jet printer, Hymarc laser, and associated computer controllers.

3.1.1 Coordinate Measuring Machine (CMM)

Generally, CMM is used for dimensional measurements in three dimensions, and is controlled by its associated computer-based motion control system. It is widely used for high accuracy verification between products and their design with help of

specific CAD software.

A CMM is not only used for quality verification purpose but also for reverse engineering. In this thesis, it is achieved from mounting laser scanner and probe head onto the CMMs, and extended to include an ink-jet printer head. The processes produce a digital geometric model from an actual part, and accurately apply an image on the final product.

The CMMs, employed for this project, are DEA IOTA model 1102 and model P [35]. They are both typical bridge type CMMs that consist of a bridge supported by legs for each machine on both sides. The two legs of the bridge are driven along the x-axis. A middle column, supported by the bridge, can be controlled to move along y-axis and z-axis. The tables of both CMMs are made of granite to ensure system stability. Figure 3.1 shows two CMMs that are used.
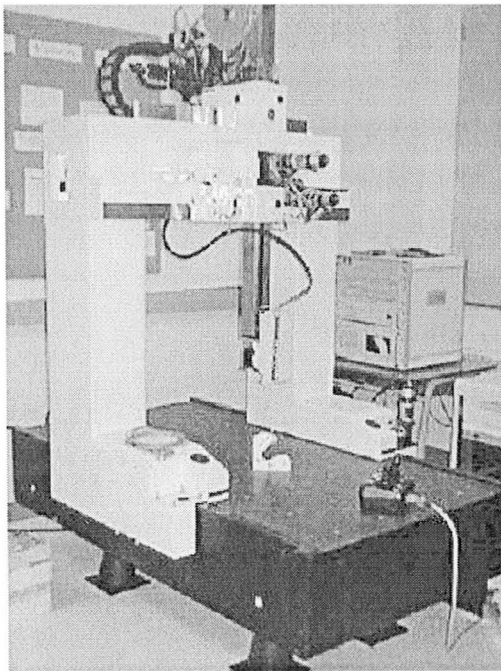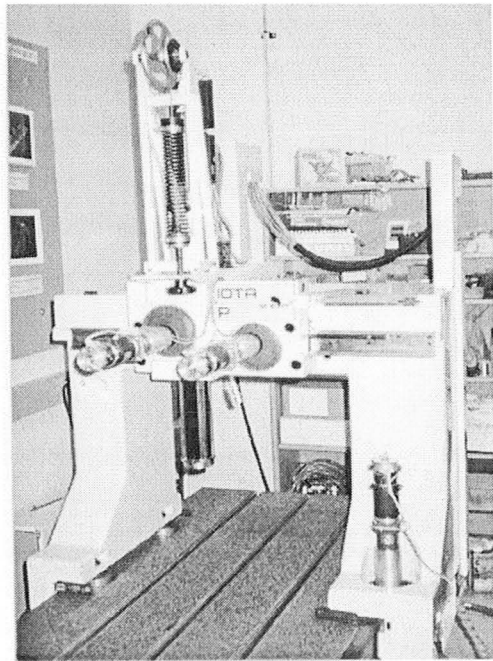
a) DEA IOTA Model 1102   b) DEA IOTA Model P

Figure 3.1 Employed Coordinate Measuring Machines

3.1.2 Serial Ink-jet Printer Head

The ink-jet printer is the device that is mounted to Renishaw PH10 probe to perform actual printing task. It contains major components of HP 51604 thermal ink-jet cartridge [37, 38], SX-28AC/SS based micro-controller circuit board programmed with associated firmware, and the mounting assembly.

The currently employed HP 51604 thermal ink-jet cartridge, shown in figure 3.2, is a 96 (Dots Per Inch) DPI monochrome device that is available to print single black color. The major aspect of the printer to be chosen is non-contact "drop-on-demand" thermal printing trait [37]. The optimal condition for the gap range is 1 ± 0.5 mm above the ink-applied surface [37, 39]. The ink in the cartridge is applicable for most porous surfaces, such as woods, fabric, paper car boards, etc, but not suitable for ABS plastic and some fine finished metal surfaces. Pre-coating for these materials is required, and will be described later in the thesis.

The cartridge contains a series of 12 linearly aligned nozzles as figure 3.2 b) shown. Since the printing signal generated from controller is serial pulses, the time that required for all 12 nozzles to perform one print of a dot row is around 30 µs. Total time for one step of firing 12 nozzles, including system waiting and delay time, is 800 µs. These time requirements restrict the print condition to be static, otherwise, row deformation and drifting can occurs.

Nozzle firing is controlled by pre-programmed SX-28AC/SS based micro-controller (see figure 3.3 a)) [40]. It is connected through 4-pin standard USB to a power supply and data connector. The pre-programmed firmware written in high-level SX/B language can be modified in an external editor and then uploaded to the 20 megahertz SX-28AC/SS micro controller using a 4-pin header. It allows user to format printing characters, load text strings and graphs, and print in a commercial way. A functional diagram of the board is shown in figure 3.3 b).

The mounting assembly bracket mates printer head onto Renishaw PAA1 adaptor [36] of PH10 probe. Geometric errors caused from this installation are corrected through system calibration, as described in section 4.6.5.
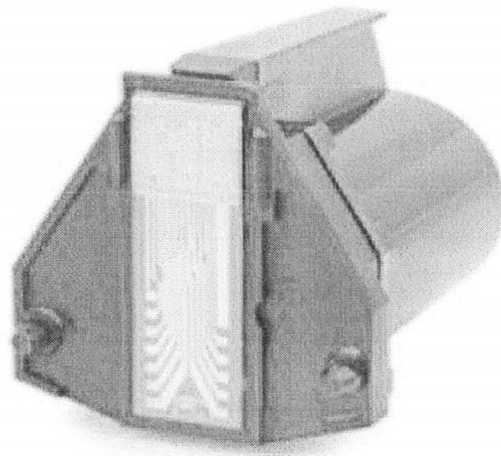
a) Real Object of HP 56104
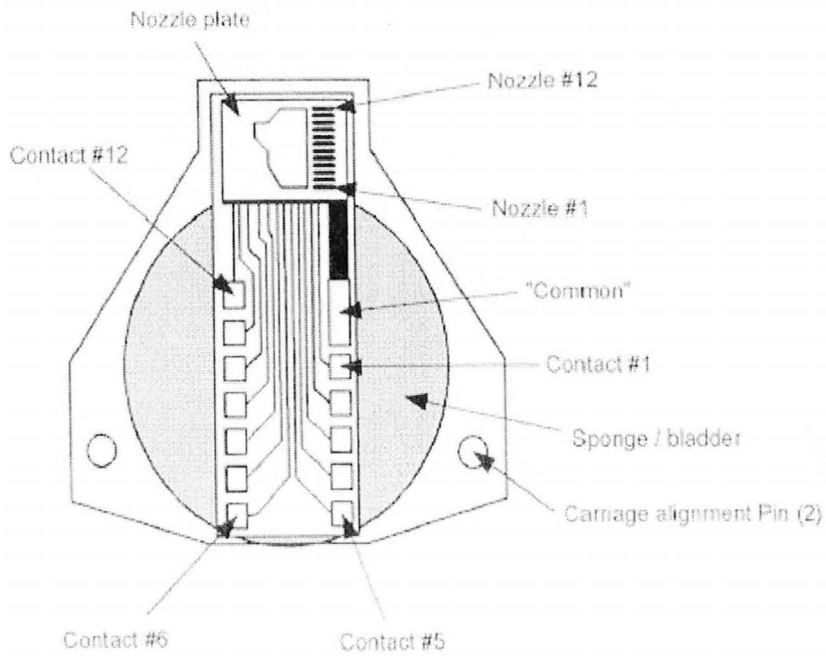
b) Bottom Surface Sketch

Figure 3.2 HP 56104 Cartridge for Ink-jet Printer [39]
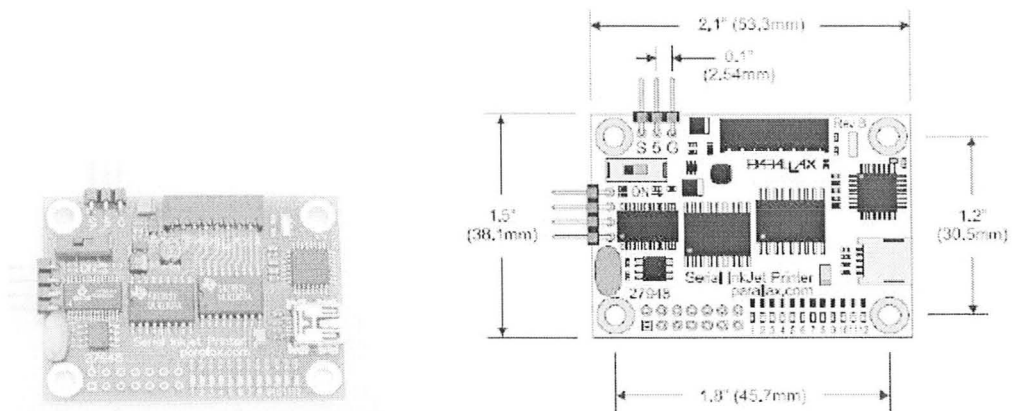
a) SX-28AC/SS based Micro-controller Circuit Board
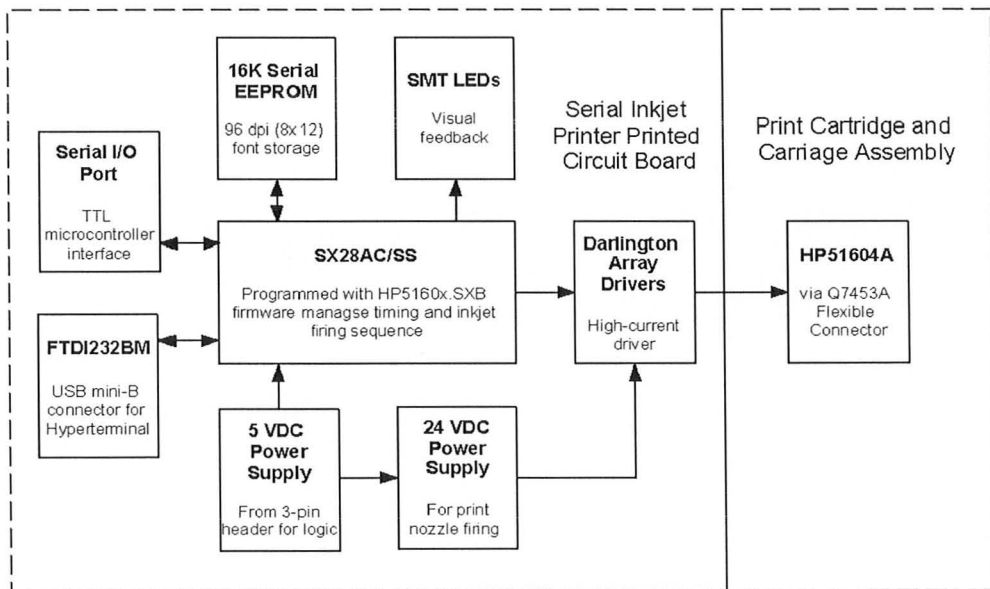
b) Functional Block Diagram Diagram of Micro-Controller

Figure 3.3 Serial Ink-jet Printer Kit [40]

3.1.3 Renishaw PH10M Motorized Probe Head

The Renishaw PH10M [36] is a motorized probe head device that expands the degree of freedom of system orientation from original 3-dimension to a 5-axis oriented system. The PH10M head is cable to rotate along phase A and B, which is

depicted in figure 3.4. The rotation specification on phase A is [0°, 105°]; and it is [-180°, 180°] on phase B (see figure 3.4 a)). The smallest rotation step that can be applied is 7.5°. PH 10 probe head achieves very high repeatability as 0.5 μm with the installation of touch probe [36]. Therefore, this error effect can be totally ignored in this thesis.

a) PH 10M

b) PH10 with Touch Probe
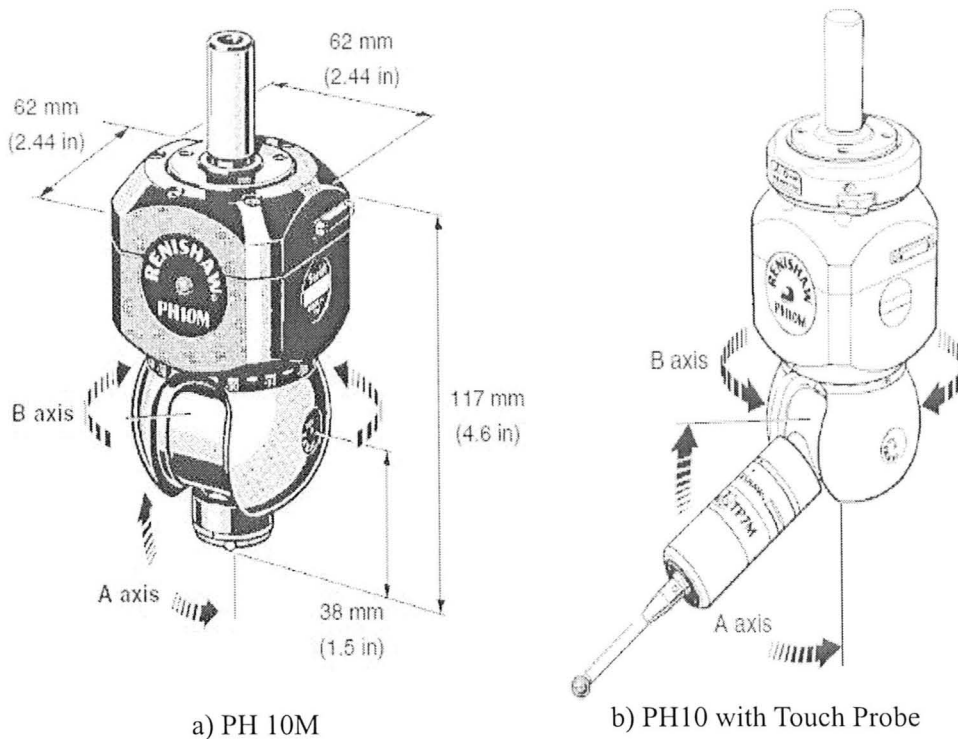
Figure 3.4 Renishaw PH10M Probe Head [36]

Replacing the printer head by touch trigger probe, CMM performs the regular measuring purpose with high repeatability. Replacement of the touch trigger probe is applied to accurately establish relevant coordinate system and product verification in this thesis (see figure 3.4 b)).

3.2 Systems Architecture

3.2.1 CMM-Hymarc Laser Digitizing System

Figure 3.5 explains system architecture with the connections. The system contains 5 major components, CMM, OTC5000 Controller, QNX based Hyscan controller, 45C/SC2 Hymarc laser camera and workstation. The workstation is an interface computer with Windows XP operating system, where utilized software has been installed. OTC5000 control box, as the CMM motion controller, uses Pentium I 133 MHz microprocessor based computer with Phar Lap ETS operating system. The OTC controller contains motion interface card that based on an 8-axis Servo-To-Go card. It monitors any CMM motion and head position from feedback signals and sends them to a Pulse Width Modulated (PWM) DC motor servo amplifier in OTC5000 to transfer the signals to CMM. The input is connected not only to workstation through Ethernet but also to the remote joystick control unit.

The Hyscan controller for the camera head is a QNX [41] operating system based Pentium computer that is connected to workstation from Ethernet as well. The controller offers intensity I, (U, V) and θ (see figure 2.2). To obtain global coordinates, recorded data needs to be sent back to CMM controller to compare with the instantaneous position of CMM arm, as well as the orientation conditions of the digitizer. The final data is transmitted through Ethernet to workstation for graphical plotting.

The capability for digitizing, motion and orientation of the laser digitizer system is illustrated in figure 3.6. If the Stand Off represents the proper gap between camera head and object surface, the camera is only able to record surface geometry within Field of View (FOV). CMM automatically moves the laser camera along x, y, z-axis, however, camera orientation requires manual adjustment as figure 3.7 shown. This mount is designed with 15° incremental pin-lock clock face plate.

This CMM-Hymarc laser digitizing system has a working volume of 750mm × 500mm × 450mm along x, y, z direction. The measuring error is as small as 13μm for one sigma distribution, which includes variations of digitizing and CMM movement [42].
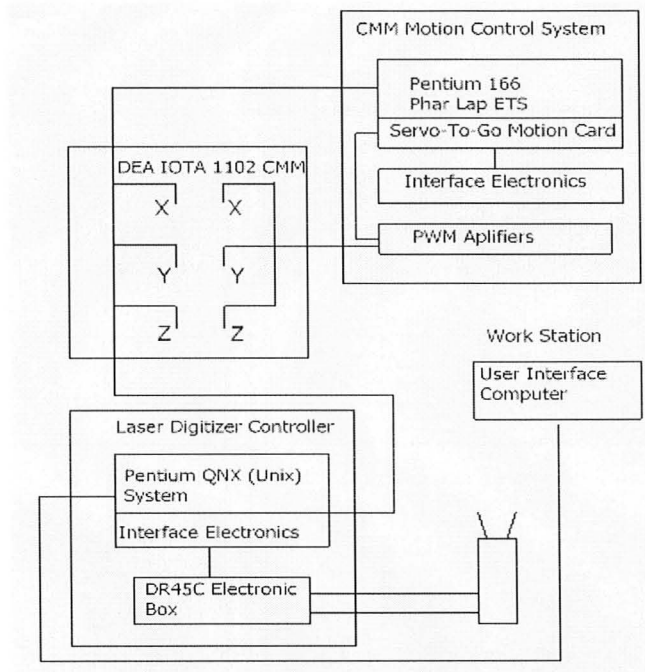
a) System Architecture
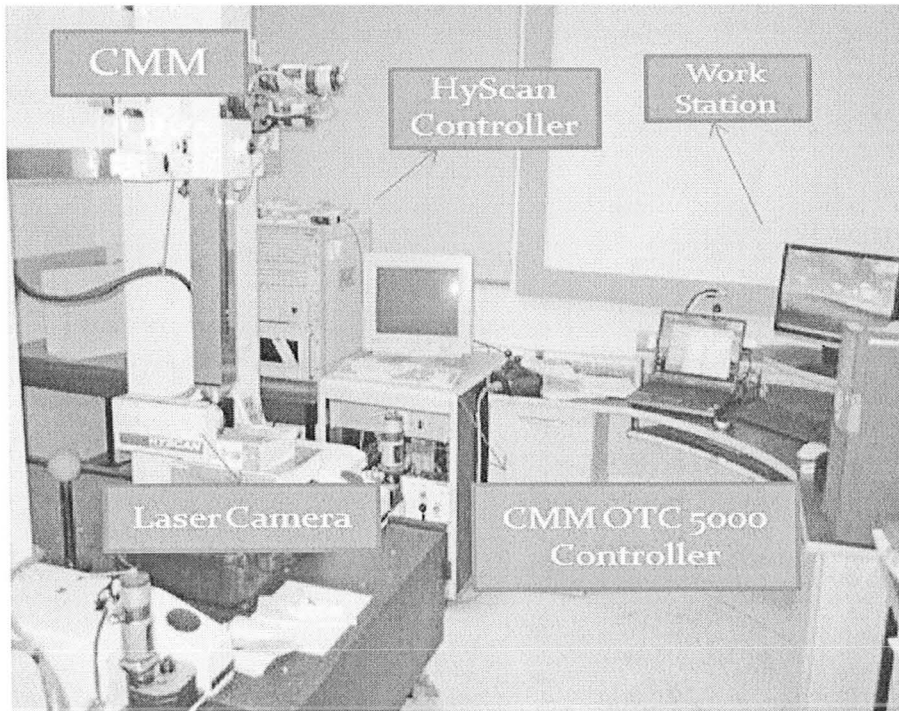
b) System Settlement

Figure 3.5 Architecture of CMM-Hymarc Laser Digitizing System
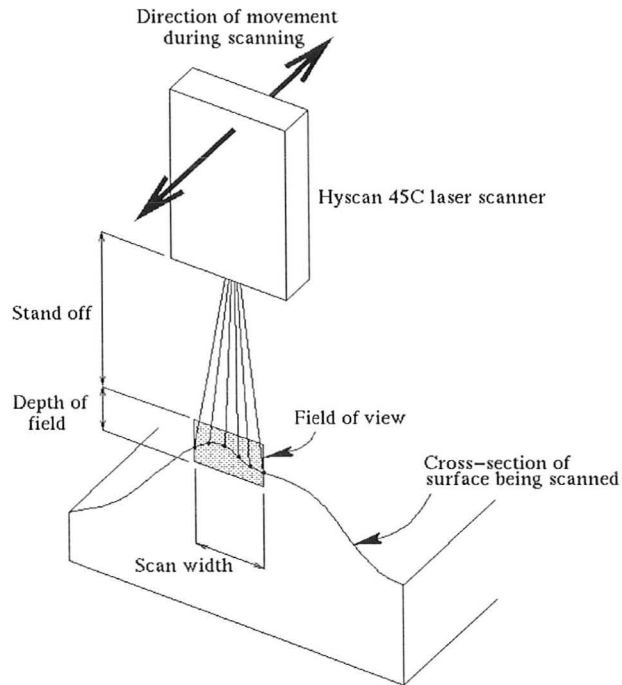
Figure 3.6 Scanning Motion with Field of View [7]
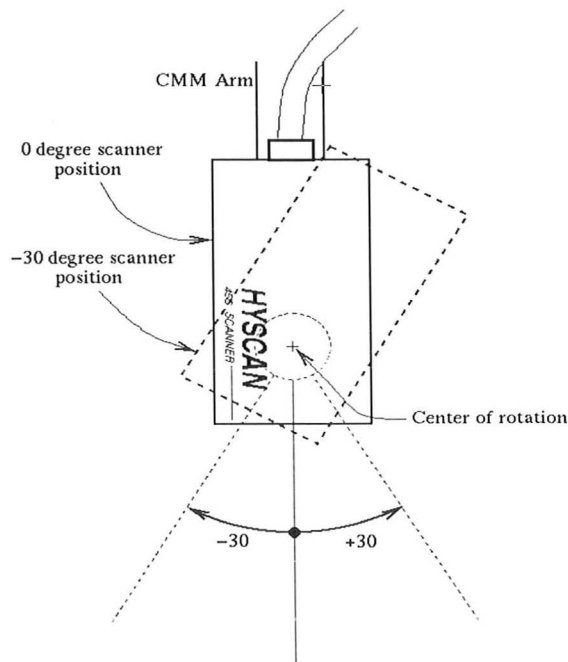
Figure 3.7 Camera Head Orientation with Trunnion Mount [7]

3.2.2 Oriented 3-D Ink-jet Printing System

The existing system architecture and general installation for the oriented 3-D printer shown in figure 3.8 is composed of major parts as workstation, CMM, ink-jet head. The workstation, with Windows XP environment, is connected to the CMM controller via an Ethernet to move the CMM and Renishaw PH10 probe. It also connects to the ink-jet head through a virtual serial port via a USB cable. The serial connection allows the communication between the interface computer and ink-jet head, so that user can program image pattern, loading the separated pattern strings and initialize the image display.
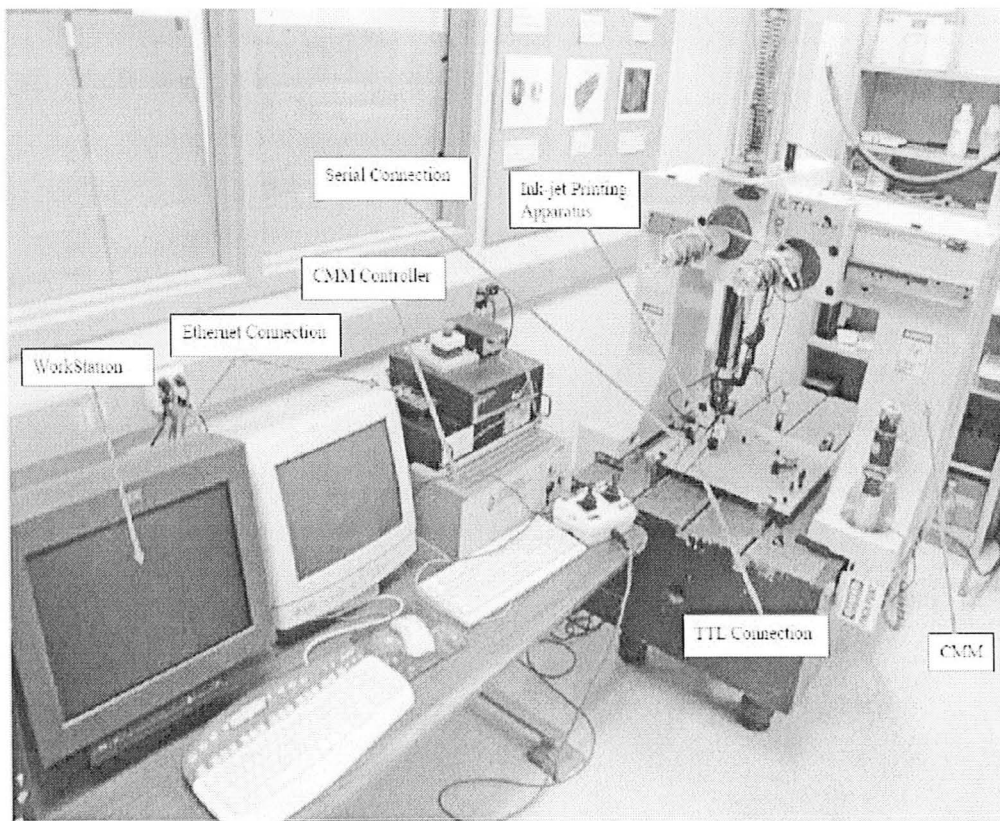
Figure 3.8 System Settlements with Connection for Oriented 3-D Ink-jet Printer [3]

The CMM controller has a TTL connection to the ink-jet head. When source code is modified in workstation and sent to OTC5000 controller via Ethernet, CMM communicates separately to printer head through TTL. After the image has been loaded CMM receives TTL logic signal from modified source code to perform designated motion of acceleration, deceleration, or remain constant speed. In this thesis, CMM moves step by step with cumulative distance of 1/96 inch to be consistent with resolution during print of single set of image strings. Each action of string dots deposition is triggered by each accomplishment of the CMM steps.

Chapter 4

Implementation of Production Workflow

4.1 New Product Development Workflow

This chapter describes a full new product development workflow. An artistic peppershaker, as a sample product, is developed from an aesthetic hand crafted model to its final rapid prototype product with reproduction of surface decoration. Generally, a peppershaker clay model with surface decoration is made by hand and laser digitized from CMM-Hymarc laser digitizing system. Then, CAD model and decoration image are simultaneously reproduced from digitized object surface point cloud data (PCD). The surface geometry is transferred for rapid prototyping. Re-engineering of surface decoration is achieved by previously established oriented 3-D ink-jet printing system. Figure 4.1 illustrates the details of the workflow with all corresponding computer tools and established equipment that are used in the workflow.
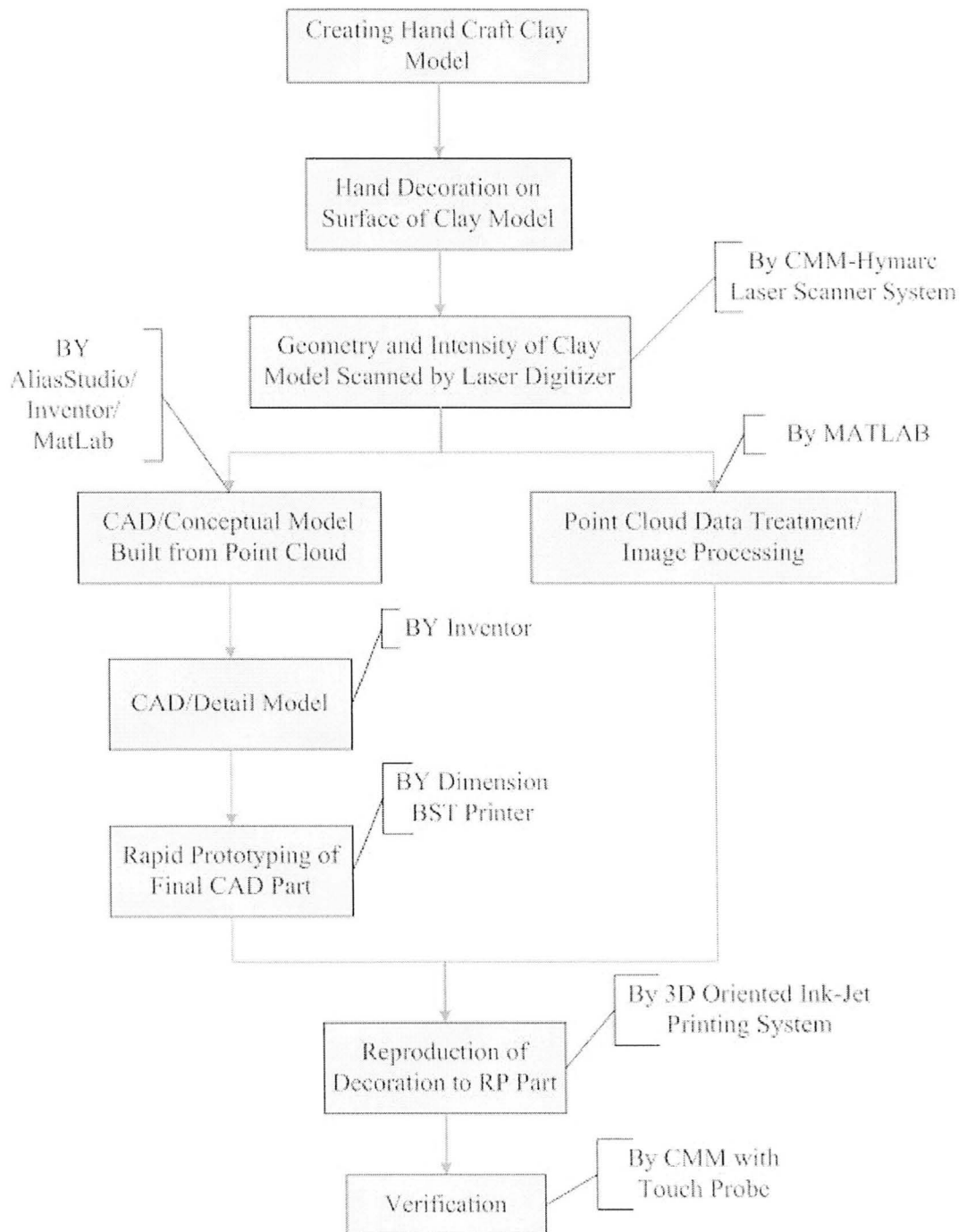
Figure 4.1 Product Implementation Flowchart

4.2 Realization of Hand Crafted Art Model with Surface Decoration

Usually, at early stages of new product development, object models are manually built up by a skilled worker or artist. The material for a model can be wood, wax, clay, etc, so that it is easy to be shaped. Our hand crafted art model was made of Crayola air-dry clay [43]. In order to facilitate laser digitizing and printing processes it is necessary to build the clay model into two halves along the symmetric mating plane (see figure 4.2).
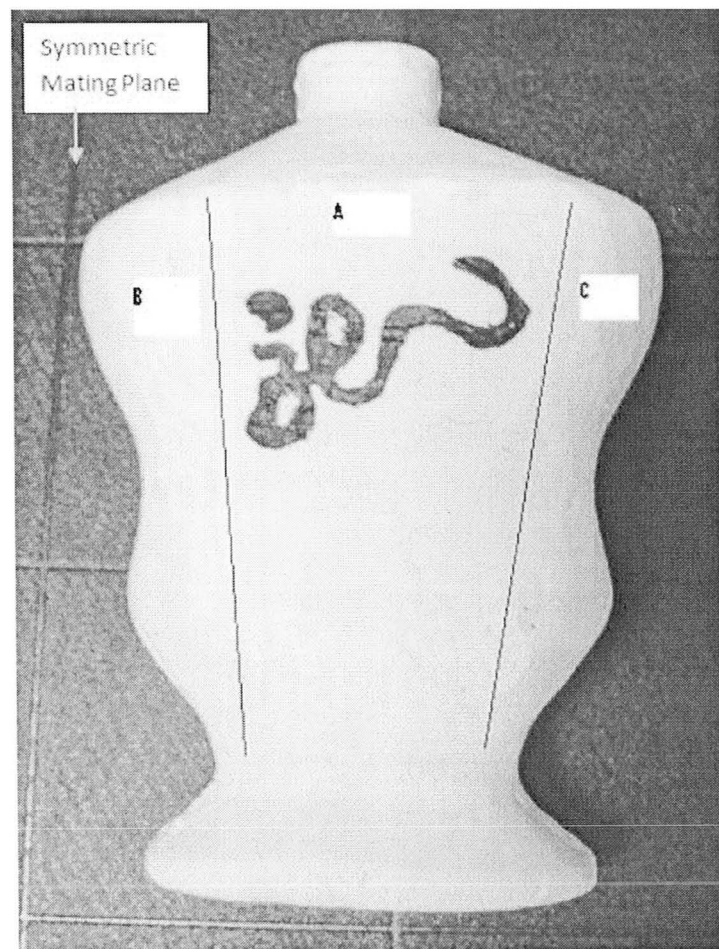
Figure 4.2 Clay Model of Half Product Body

Due to poor surface condition of the clay model, the decoration region of the body surface needs to be pre-coated to avoid the ink bleeding along surface porosities and cracks. Before any surface hand decoration InkAID washable white matte [44] is applied on the surface. In addition, this white pre-coat can enhance decoration contrast to facilitate the laser digitizer to distinguish image background and foreground. An aesthetic hand-drawn black-ink Chinese character was decorated on the major surface of the object in this case. The character means dragon.

4.3 Laser Digitization of Hand Craft Art Model

The CMM-Hymarc laser digitizing system has been set up to collect object surface coordinate values, simultaneously with their correspondent surface intensities. The Laser digitization of clay model generates the point cloud data (PCD) of object geometry, which offers a CAD reference for product CAD model design. The image of decoration can be constructed from recorded information.

4.3.1 Strategy of Digitization and Environment

The ideal digitizing plan is to set up a proper intensity collection range for the laser digitizer and collected object geometry simultaneously with intensity information. The advantage of this scanning process is quite apparent that the process is not only simple and efficient but also able to precisely address the intensity levels to their exact positions.

For future CAD model construction and image processing, it is the same PCD that is treated. Also, for the image processing purpose, CMM feeding speed of the laser digitizer needs to be adjusted to a suitable level to meet the specification of printing resolution.

The setup of digitizing system and its local coordinate system are shown in figure 4.3. A simple part jig, with three datum standoffs and a steel ruler, is used to position the digitizing part of the peppershaker. It is used to create the local relevant

coordinate system for decoration reproduction, and it is discussed in section 4.6.2 for details. The centre of the calibration ball is the origin of local coordinate system.
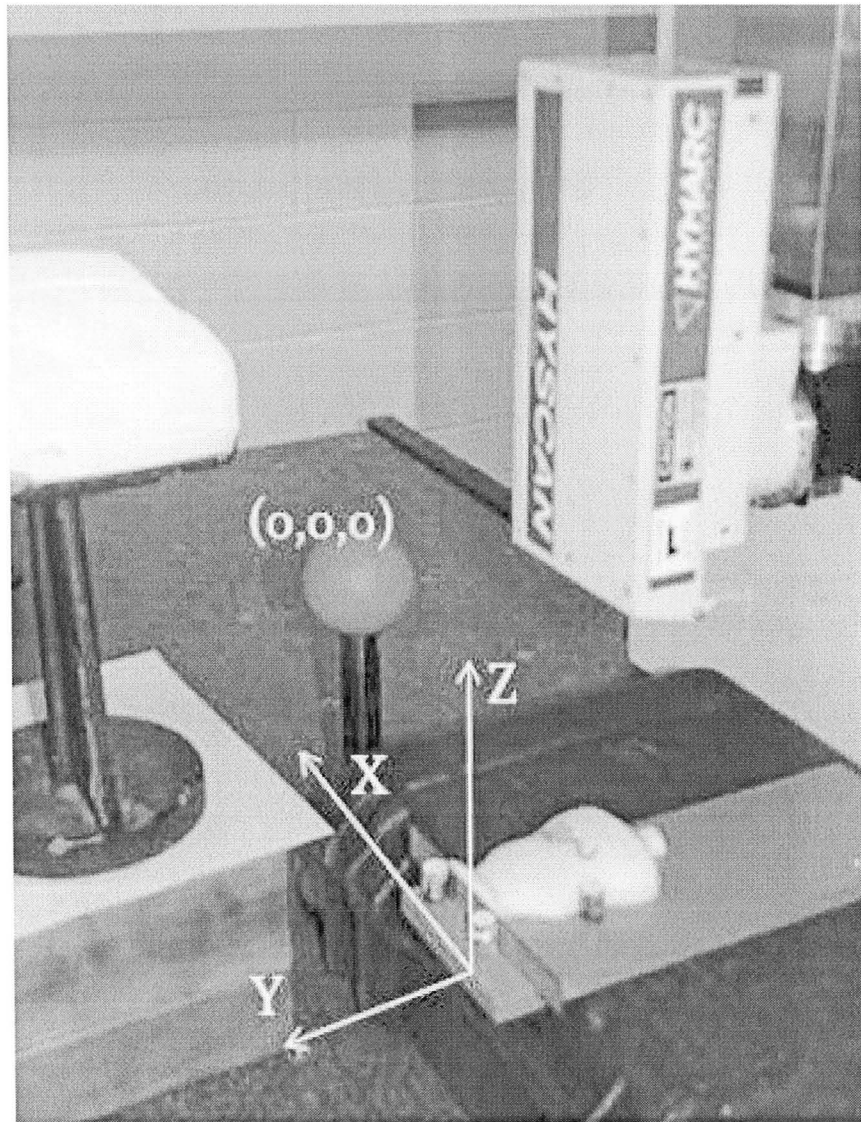

Figure 4.3 Scanning Status and Part Jig

Laser digitizing shall always be performed in dark room if the intensity needs to be collected as well as the surface geometry. This is because any illumination creates the noise to intensity value. The intensity collection range for the digitizing system is set up to be:

$$I \in [0 \quad 350{,}000]$$

4.3.2 PCD Results

For the digitization that contains intensity, the laser digitizer collected 930,622 points from body of the peppershaker and its fixture. The size of the default file from scanning system is more than 32Mb. It is necessary to transform the default .hym binary file to a standard ASCII [7], so that, it can be not only export to MATLAB [45] but also recognized by most CAD tools.

Collected by Hymarc camera, point could data are constructed as $t_{in} \times 4$ matrix if intensity included, and $t_{ge} \times 3$ matrix if only geometry has been recorded, where t represents the total number of the collected points. The two types of matrices can be illustrated as the following form:

For geometry only: $PCD_{ge} = \begin{bmatrix} X_i & Y_i & Z_i \end{bmatrix}$, where i = 1, 2, $\cdots$ t_{ge}.

For geometry with intensity: $PCD_{in} = \begin{bmatrix} I_i & X_i & Y_i & Z_i \end{bmatrix}$, where i = 1, 2, $\cdots$ t t_{in}.

4.3.3 Digitizing Issues for Image Processing

The slowest CMM feeding speed that can be adjusted is $V_f = 0.33$mm/sec; the digitizer frequency $f_s = 3.3$Hz. Theoretically, the distance between the two scan lines can be calculated as the following:

$$D_{ave} = \frac{V_f}{f_s} \approx 0.1mm$$

In order to facilitate the data simplification processes, the distance between adjacent points along two primary directions within the image region shall be narrowed to less than 0.264 mm (1/96 inch). Measurement verification shows the distances between two scan lines within one scanning process the values are validated within an approximate range of 0.1 ~ 0.2mm. In addition, the digitizing speed along

scan line direction is 0.1 mm/sec. From this scanning process, the density of the achieved PCD is approximately 10 points/mm (see figure 4.5). The result PCD is acceptable.
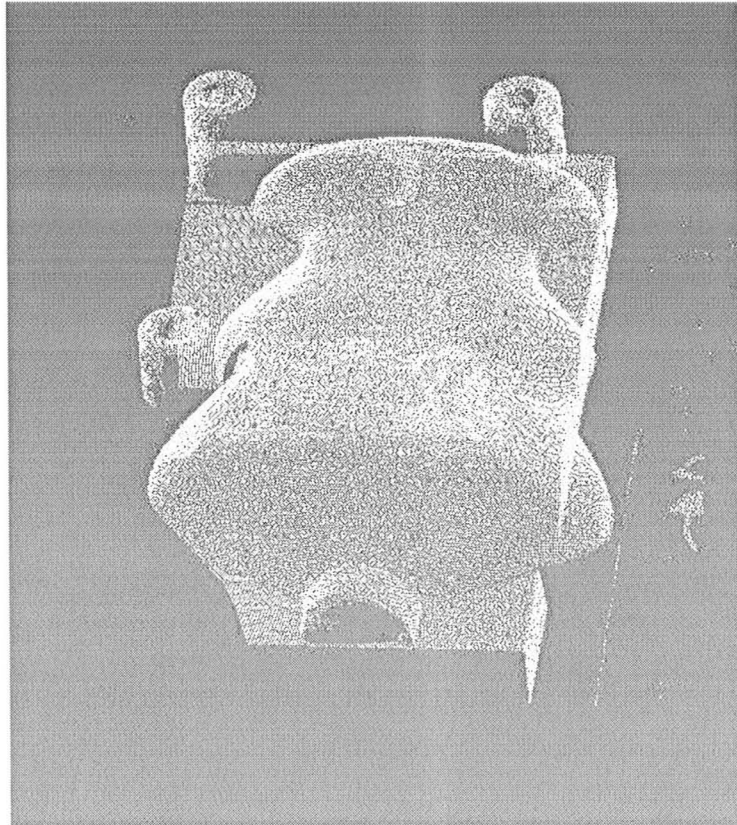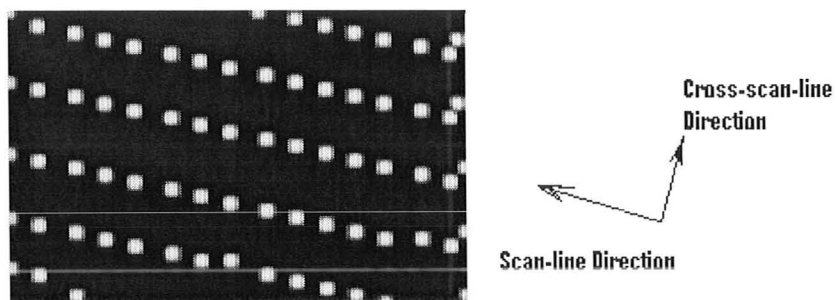

Figure 4.4 Result of Collected PCD

Figure 4.5 Collecting Points along Scan Lines

4.4 Implementation of CAD Model

Implementation of CAD model includes two stages, generation of conceptual model and detailed model. Any geometric demerit can be improved by changing the design shape at the conceptual stage without creating implementation problems in later stages. The thickened CAD model will be exported to rapid prototyping machine for production of the real part.

4.4.1 Generation of Conceptual Model

The processes of generating product concept model are illustrated in flowchart of figure 4.6. The main edge portion of the point cloud data are extracted and sampled for applying B-Spline fitting method to generate the more simple main edge curves with allowable tolerance. Product body surfaces are constructed based on edge curves. Verification is necessary to ensure consistency between new created CAD surfaces and object point cloud data. For convenience and quality reasons, inspection points can be settled for both curve and surface checking.

Point Cloud Data extraction

To process the point cloud data, ImageWare (version 11) [26] is used as CAD tool. The point cloud data is extracted and sampled. For late oriented image printing purpose, the main body surface must be consistent with final digital model to perform accurate print. The product body is analyzed to define main surface and the edge curves of it. In addition, extracting and sampling for the edge curves can be performed (see figure 4.7). The extracted data is transformed to ASCII file for further processing.
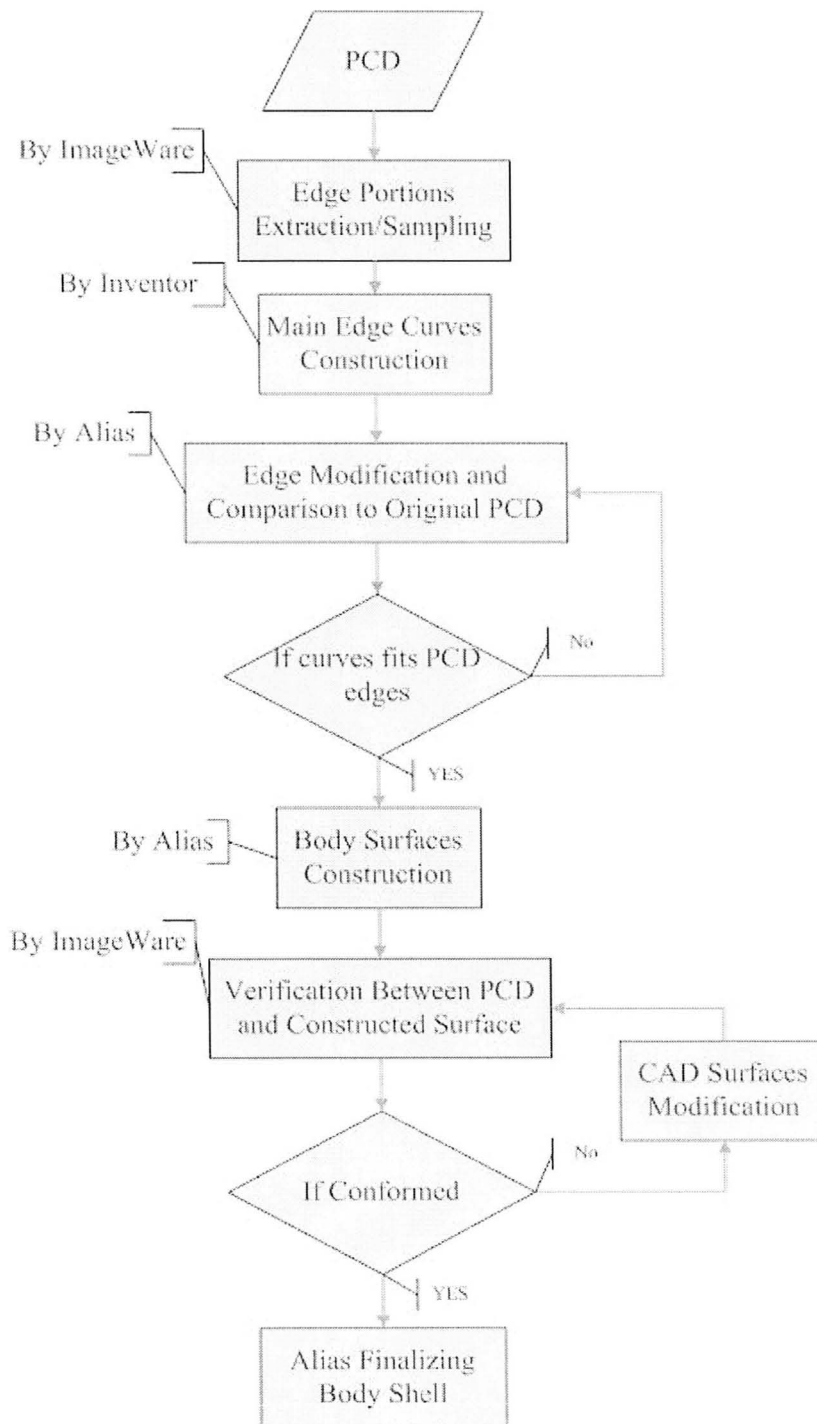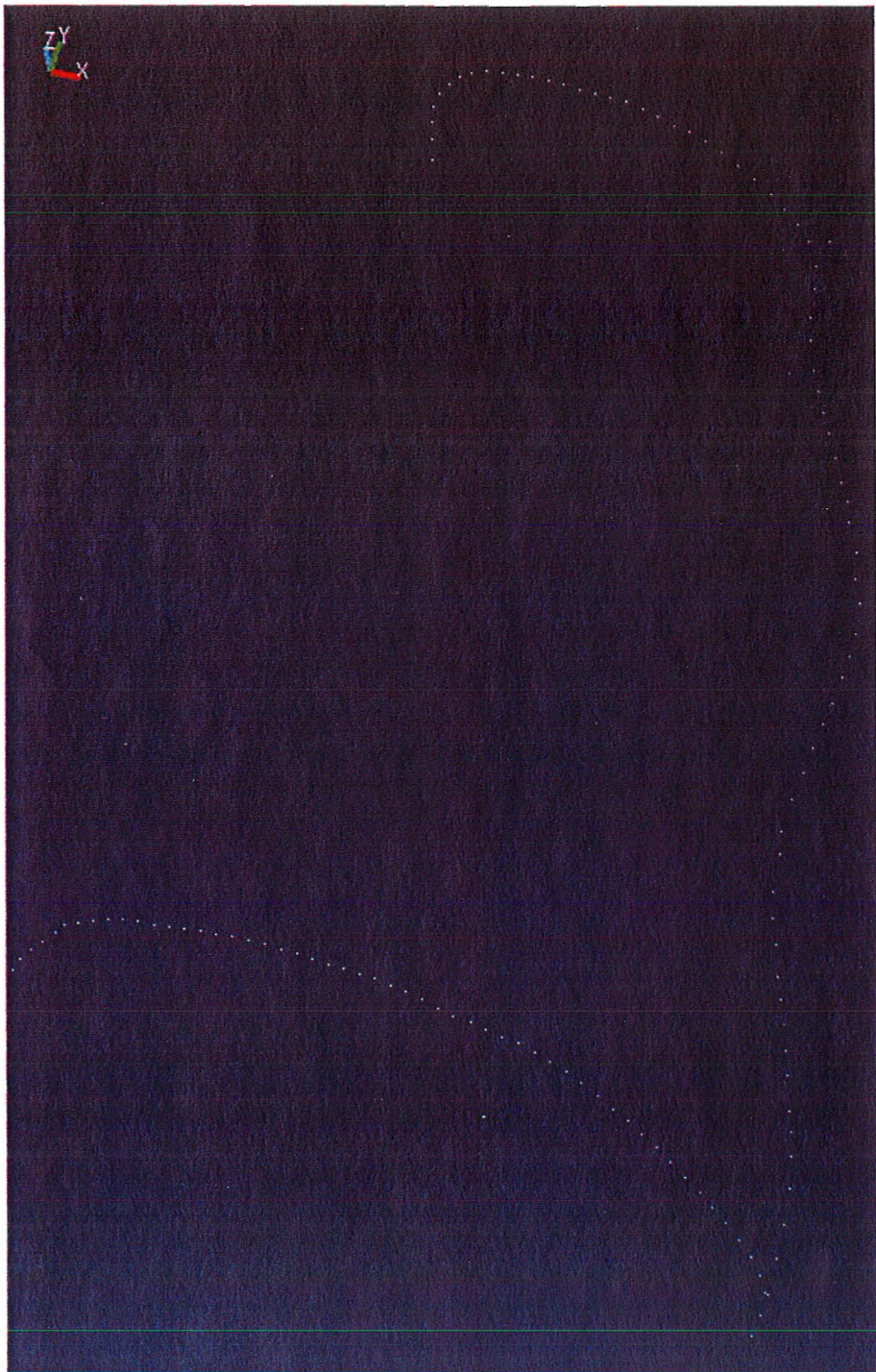
Figure 4.6 Process Flowchart for Conceptual Model

Figure 4.7 Curves Point Cloud Extraction

Main Curves generation

The edge curves of the main body surface are the key for constructing an accurate CAD surface. Enclosed edge curves for the surface can be regarded as B-Spline curves. With provided MATLAB code, application of *Uniform Parameterization Least Squares Algorithm* [32, 33] returns the actual B-Spline curves.

By simply entering the number of the sample points and their geometric values, the least squares fitting method reads the sampled curve points and calculates the actual control polygon for a simplified B-Spline curve. It also generates all defined sample points along actual curve to facilitate user to draw the real curve. Calculated residual error provides a reference to depict level of difference between profiles of sampled points and constructed curve. In this case, all MATLAB solutions of B-Spline are listed in figure 4.8 a)-c), and all sampled points are imported to Inventor or AliasStudio [27] for construction of real B-Spline curves. All residual errors are controlled to be less than 0.4 mm.

Furthermore, all end points of curves shall lie on object mating plane for proper shaping. The mate plane is defined as the first datum plane for CAD model design and for decoration printing, which is consensus to the upper surface of the part jig steel plate. To guarantee no sharp edge for final product, all ends of upper and lower profile edges shall be modified to be perpendicular to the first datum plane (see figure 4.8 d)).

By exporting the curves and original point cloud data into AliasStudio, it is able to finalize all curves so that they are conforming to clay model shape (see figure 4.9). Manually alignment between the curves structure and original point cloud data is performed to create conformity curves and surfaces, and to assure a appropriate surface verification.
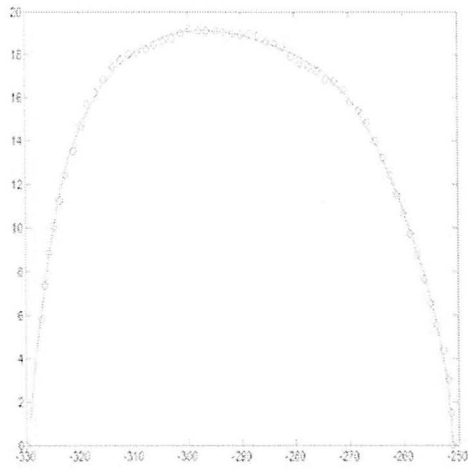
a) Upper Profile Edge
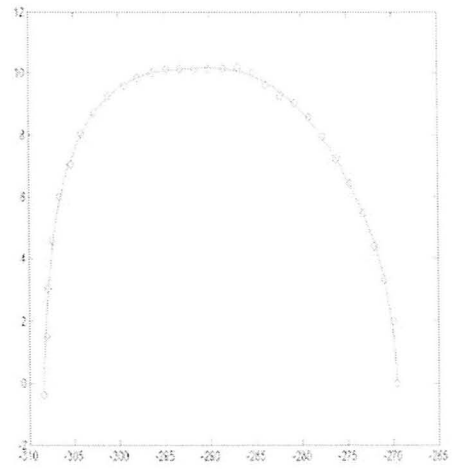
b) Lower Profile Edge
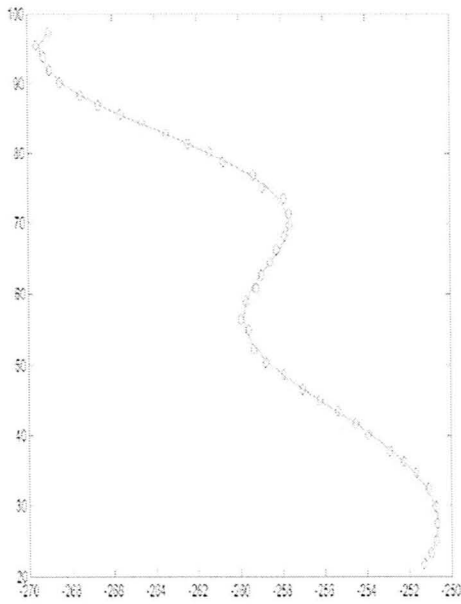
c) Side Edge
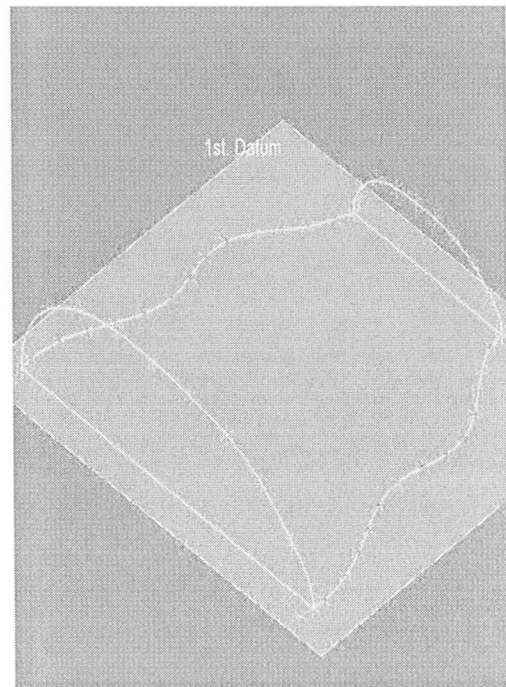
d) Edges of Main Body Surface

Figure 4.8 Construction of Main Body Edges (All Units in mm)
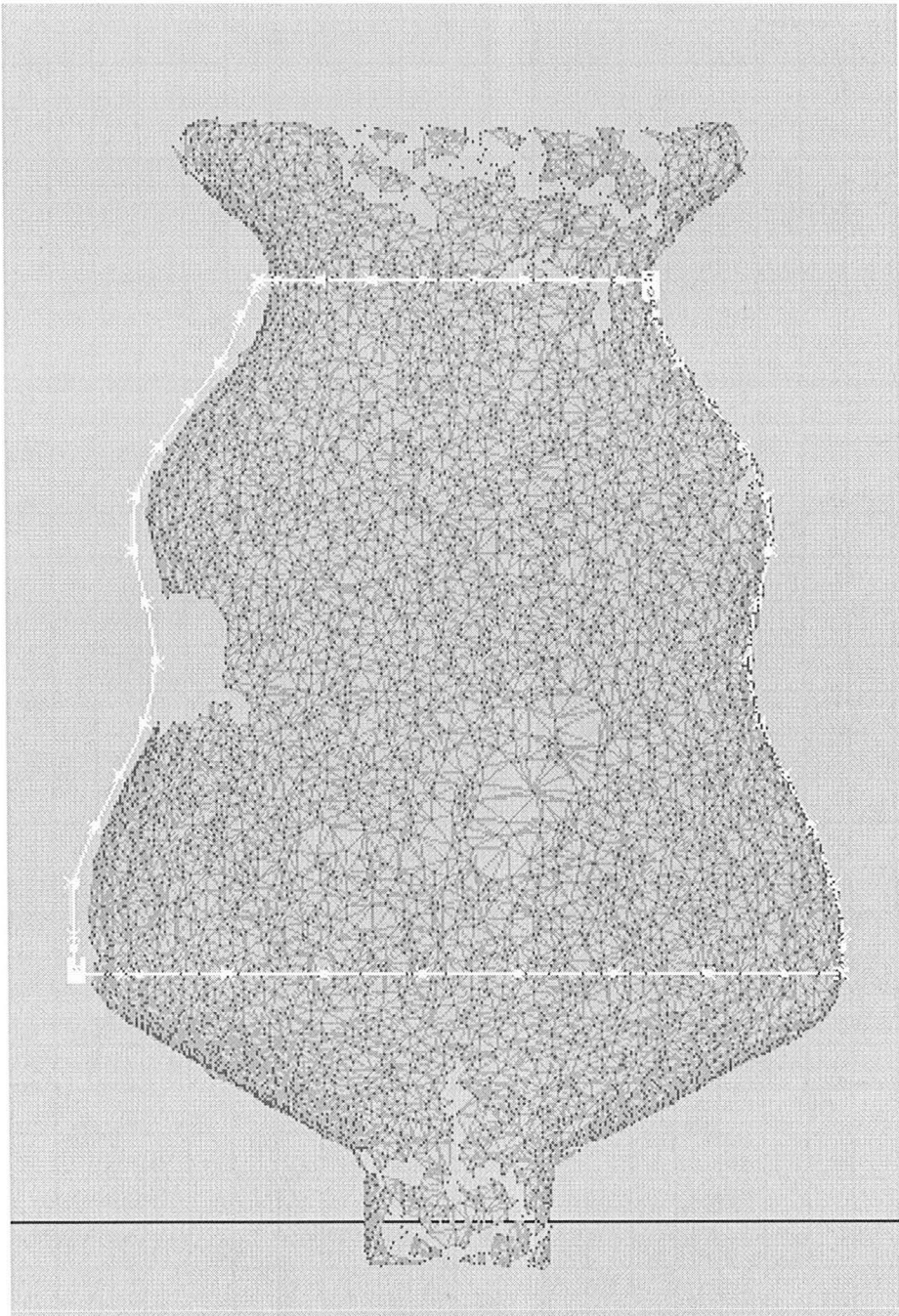
4.9 Modification and Alignment of Main Edges

Surface forming with Modification

All major surfaces of the product are constructed from demonstrated significant edge profile curves in figure 4.10 a) by AliasStudio. The major body for the object is well-designed aesthetic smooth Coons patch surface with relative flat area 'A' that locates at the middle portion of the object. The purpose of this design is to meet the criteria of printing system. To achieve this design, instead of constructing a traditional two directional B-Splince surface, AliasStudio provides 'Square Surface' function that allows us to create a Coons patch surface [29] that has difference influence level from boundary edge curves. From figure 4.10 b), the three sections of major patched B-Spline surface is consistent with the design of clay model. Also, adjustment and the modification of the Coons patch surface can be applied by change of the surface CV hull.
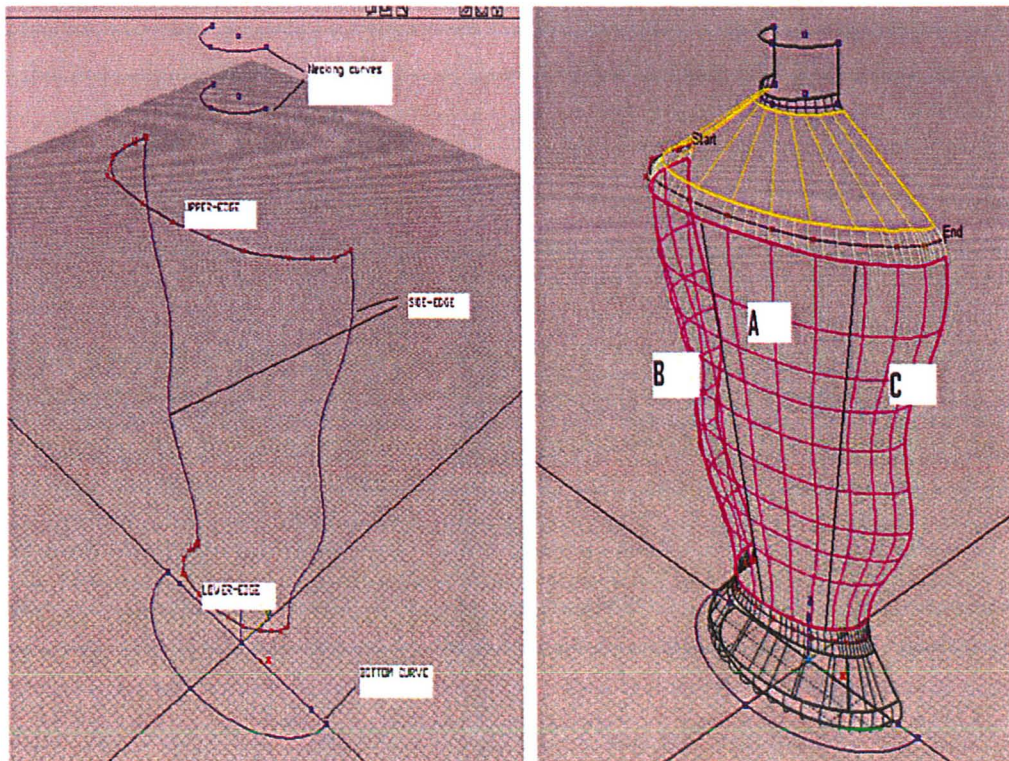
a) All Body Edges   b) Constructed Body Surfaces

Figure 4.10 Body Surfaces Construction

Verification and Result

The conformity verification between conceptual CAD model and clay model is significantly vital for decoration reproducibility. Knowing the optimal tolerance of ink-jet printing status the surface decoration area shall be adjusted to achieve as less difference as 1mm. ImageWare, as a CAD tool, is recommended to perform the verification task due to reasons of accuracy and better operational convenience. The verification can be achieved through the alignment between original point cloud data and created conceptual model. Modification of object conceptual model is required only if the error exceeds allowable tolerance.
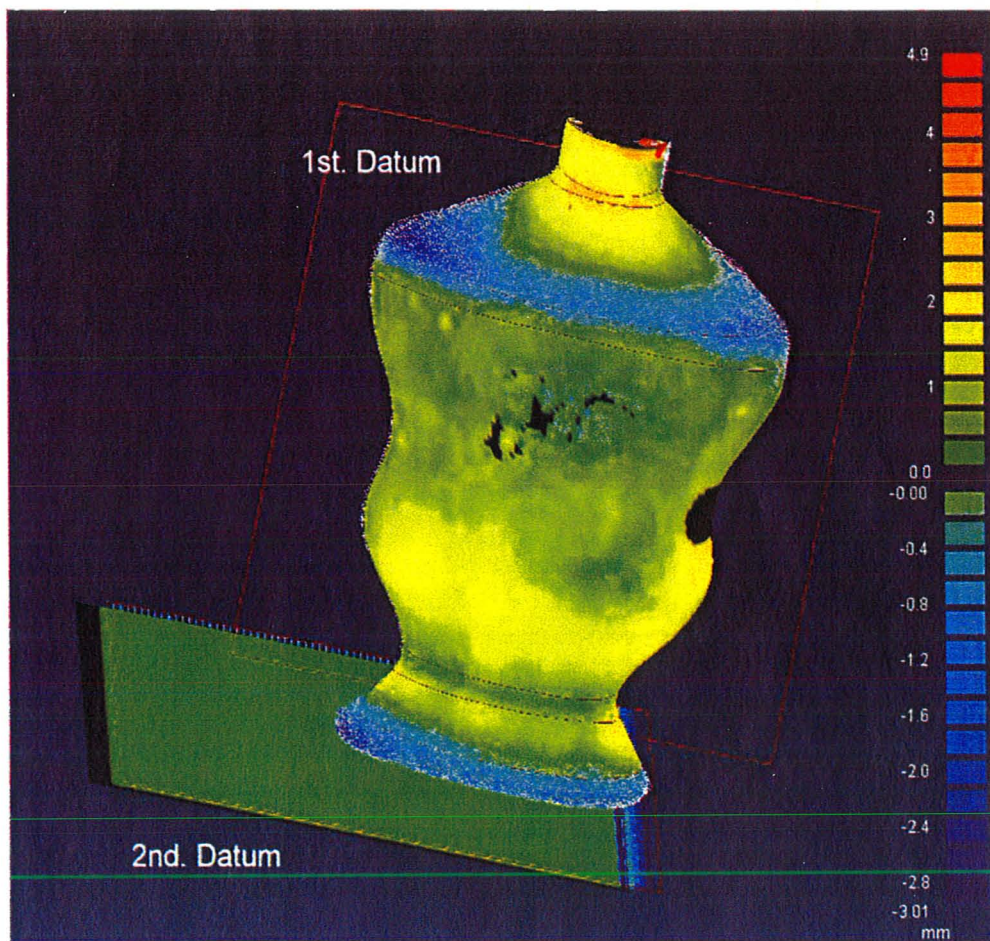
Figure 4.11 Conceptual Model Verification Result

Instead of implementing automatic 'Best Fit' alignment [26] that has been provided by Imageware, manual alignment is executed because it can assure successful decoration re-engineering process and result. For manual alignment, some datum planes have to be defined. As we discussed before, the 1st datum plane has been defined as the object symmetric mating plane. In addition, the peppershaker bottom surface can be regarded as the 2nd datum as figure 4.11 shown. The alignment of datum planes guarantees a proper alignment process for original PCD and constructed conceptual shell. In this case, the error between the two corresponding datum planes has been narrowed to less than 150μm. The maximum deviation between original PCD and constructed conceptual shell is controlled to be less than 1mm in decoration area (see figure 4.11).

4.4.2 Generation of Solid Model with Detail Design

Detailed design of solid CAD model is obtained by Inventor 2008 version [28] through imported conceptual shell. First of all, all surfaces constructed from conceptual design are thickened to a specific value towards the inner surface. Then, the design of details, according to customer request, can be added to the thickened model. As figure 4.12 shows, we add locators, lip structure and neck thread on the solid model of the peppershaker. The lip-indentation structure can facilitate the assembly and gluing processes. The three locators are able to not only help the assembly process, but also be used for locating any local part coordinate systems with design of specific fixture.
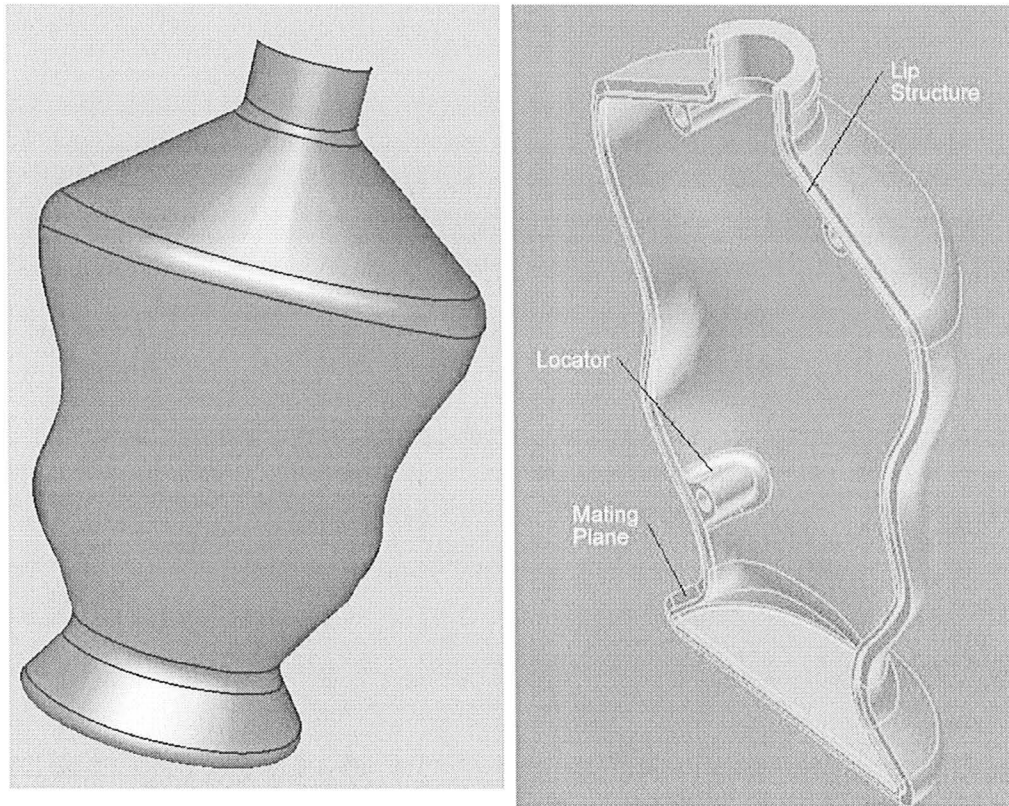
a) Conceptual Model   b) Solid Model with Details

Figure 4.12 Design from Concept to Solid with Details

Boolean Operation for Lip and Indentation Structures Design

To design the lip and indentation structures for properly engaging and mating of two half-piece objects, Boolean operation is performed in Inventor (see figure 4.12). Followings are detailed procedure for design of product lip and indentation structures:

For lip structure:

1. Create a work plane that offsets from the mating plane according to the depth of lip design.

2. Extract and project the external profile edge from the mating plane to the work plane.

3. Offset the projected edge to create two scaled-down edges profile, so

that a section profile can be sketched from closing the two scaled-down edges to extrude (see figure 4.13 a)).

4. Set the extrusion length to be slightly greater than the distance between the offset work plane and the symmetric mating plane, so that the extruded lip can fully contact to the product part.

For indentation structure:

1. Create a work plane that offsets the mating plane with certain distance.
2. Extract and project the inner profile edge from the mating plane to the work plane.
3. Offset the projected edge to enlarge it according to lip structure outer boundary; then, closed the modified edge loop.
4. Extrude this created profile loop towards the mating part to subtract an indentation with designed depth as figure 4.13 b) shows.

4.4 Implementation of Rapid Prototype Model (RP Model)

In order to rapid prototype the product, the default *.ipt* file of thickened CAD model needs to be transformed to default *.stl* file for RP machine to recognize. The result of RP model is displayed in figure 4.14.

Knowing that according to RP machine capability, the thinnest layer that can be generated is 0.01inch. With this specification of our RP machine, the product is white and plastic. Also, the surface roughness and geometric error are both around 0.01 inches (0.254mm). Due to the high value of surface roughness, the surface trait can be viewed by eyes. With different ways of product settlement in RP machine, we can have different surface traits. The surface quality can be slightly improved by choosing a good product settlement for rapid prototyping.
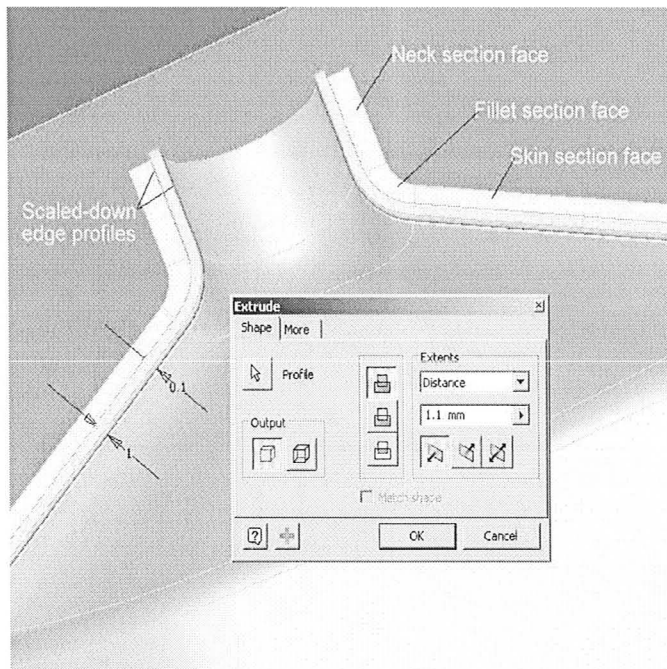
(a) Design of Lip
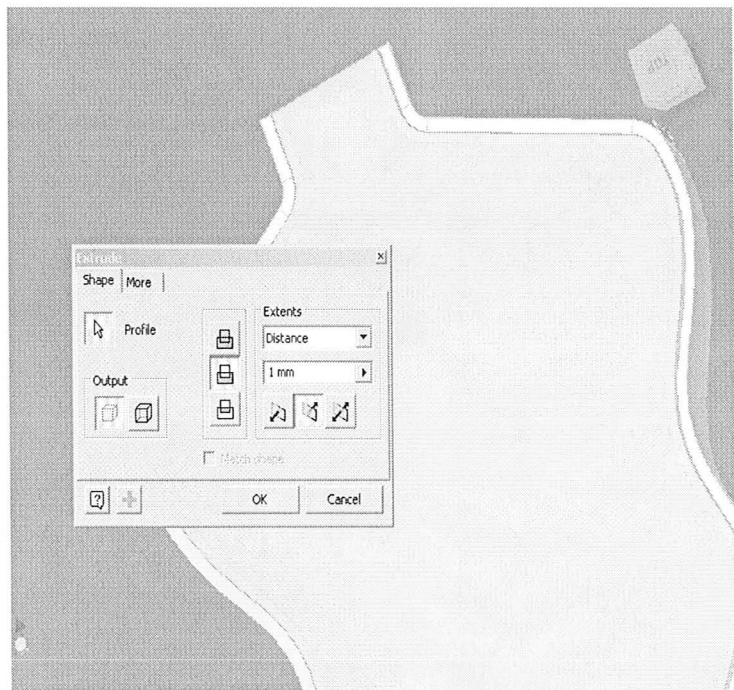
(b) Design of Indentation

Figure 4.13 Detailed Design of Product Mating Feature
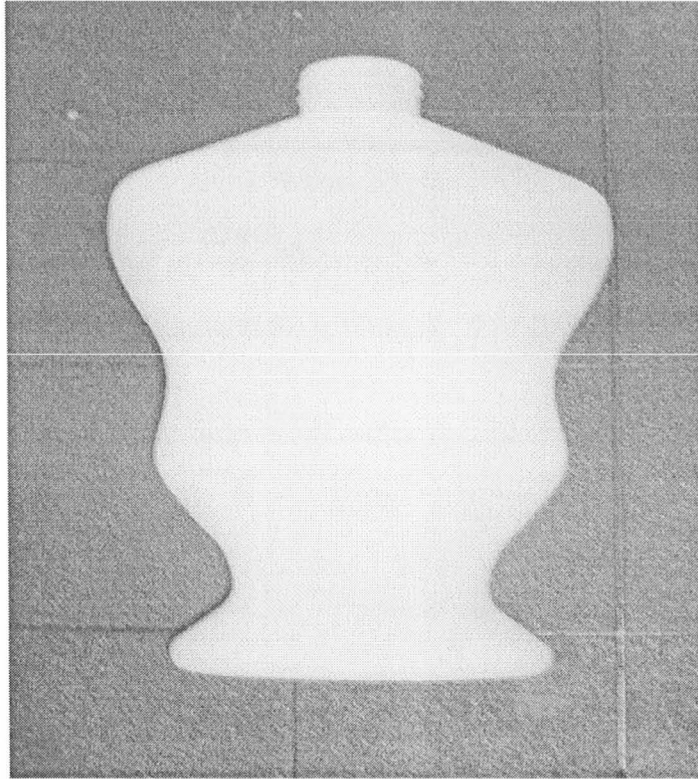
Figure 4.14 Result of Rapid Prototype Model

Pre-coating for RP Model

Adhesive problem for the ink to plastic surface occurs due to poor surface condition and ABS material of the plastic RP model. The solution of this issue is to apply suitable transparent pre-coat on printing area to achieve ink adhesion, and to avoid the ink bleeding along surface porosities and layers. Before printing, transparent wash-soluble InkAID [44] is applied on the surface. The thickness of applied coat is negligible when it is comparing to the margin of printing specification.

4.5 Image Processing

The objective of image processing is to extract the intensity information from

original point cloud data to create the required image that fits for printing on the smooth surface. The geometry information of the point could data also allows visualization of 3D locations of plotting for all image pixels. The final processed image has to be binary and the image resolution shall be consistent with printing resolution for the oriented 3-D printer.

4.5.1 Strategy of Image Processing

For original PCD, geometry and intensity values around decoration area needs to be extracted and sorted to meet the print specification and resolution. It requires simplification process for the original data due to the higher density of the original PCD. Specified in chapter 3, the ink-jet printer head HP 56104 cartridge has 12 nozzles with distance of 1/96 inch (0.264 mm) between each other. Therefore, the printing system is capable of produce image with resolution of 96 DPI. However, by roughly measuring the original PDC density, image resolution is not exactly consistent but it is around 254 DPI (100 μm). To insure the resolution consistency of the output image data, 1/96 inch (0.264 mm) shall be the restricted distance between every two pixels, both along horizontal and vertical directions in x-y plane. Figure 4.15 illustrates the details of this simplification method.

Based on those constraints, it is able to simplify the data by setting the boundary conditions on a projecting plane (x-y plane) for each defined area according to the printing resolution. For instance, set A(x(m×n), y(m×n)) to be the destination positions on x-y plane, where n = 1, 2, ⋯ N, and m = 1, 2, ⋯ M. N and M are any integers. They are regard as position number along x and y direction. Also, x,y,z are the correspondent coordinates. The defined boundary area for any A(x(m×n), y(m×n)) is:

$$Area_{(m \times n)} \in \lfloor x_{(m \times n)}, \ x_{(mxn)} + 0.264) \cap \lfloor y_{(m \times n)}, \ y_{(m \times n)} + 0.264)$$

Any point within its specified area shall be simplified as one point that is

located on the specified position A(x(m×n), y(m×n)). The corresponding z(m×n) can be calculated as the average of all z values with in this specified area. Also, the same calculation can be performed to generate the average intensity value for this position.
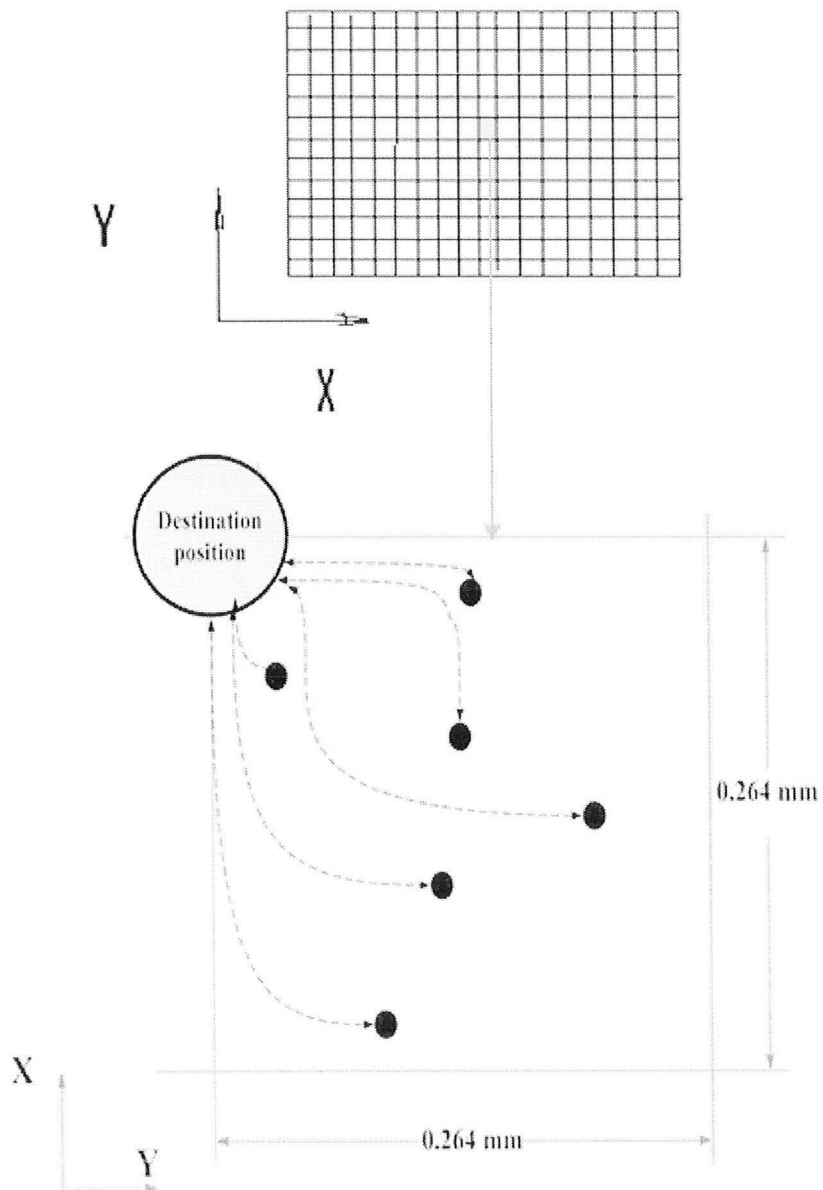

Figure 4.15 Strategy of PCD Simplification

4.5.2 Detailed Steps of PCD Simplification Algorithm

1. Estimate the rectangular image size that needs to be printed on the surface. Set the size of the image along x-y plane (object symmetric plane) equal to $l \times h$, where l and h are the length and height of the image. According to the image size, extract the original PCD_{in} to construct a new matrix $P_1 = \begin{bmatrix} I_{im} & X_{im} & Y_{im} & Z_{im} \end{bmatrix}$, where $im = 1, 2, \ldots t_{im}$, where t_{im} is the total extracted point number.

2. Set basic pixel grid size to be a $g \times g$ square. Let:

$$N = \left\lfloor \frac{l}{g} \right\rfloor, \ M = \left\lfloor \frac{h}{g} \right\rfloor$$

Let $n = 1, 2, \ldots N$, and $m = 1, 2, \ldots M$. $x_{(n \times m)}$ and $y_{(n \times m)}$ represent upper boundaries along x and y direction for any pixel grid in extracted image area with correspondent position of (m,n).

3. For $n = 1, 2, \ldots N$, and $m = 1, 2, \ldots M$, create transitional cell array Pt, so that:

$$Pt = \begin{bmatrix} Cell_{(1,1)} & Cell_{(1,2)} & \cdots & Cell_{(1,N)} \\ Cell_{(2,1)} & Cell_{(2,2)} & \cdots & Cell_{(2,N)} \\ \vdots & \vdots & \vdots & \vdots \\ Cell_{(M,1)} & Cell_{(M,2)} & \cdots & Cell_{(M,N)} \end{bmatrix},$$

$$Cell_{(m,n)} = \begin{bmatrix} I_{i(m,n)} & X_{i(m,n)} & Y_{i(m,n)} & Z_{i(m,n)} \end{bmatrix}$$

where:

$$X_{i(m,n)} \in [x_{(m,n)}, x_{(m,n)} + g], \ Y_{i(m,n)} \in [y_{(m,n)}, y_{(m,n)} + g]$$

$i(m,n) = 1, 2, \ldots t_{c(m,n)}$, and $t_{c(m,n)}$ represents the number of the points that exists in the specific cell of the array.

4. For all cells, let $X_{(m,n)} = x_{(m,n)}$, and $Y_{(m,n)} = y_{(m,n)}$.

Calculate the average values of intensity and z as the following:

$$Z_{(m,n)} = \frac{\sum_{i=1}^{t_{c(m,n)}} Z_{i(m,n)}}{t_{c(m,n)}} , \quad I_{(m,n)} = \frac{\sum_{i=1}^{t_{c(m,n)}} I_{i(m,n)}}{t_{c(m,n)}}$$

Then, simplified point cloud data can be represented as new cell array P_s:

$$P_s = \left\{ \begin{array}{ccc} \left[I_{(1,1)} \quad X_{(1,1)} \quad Y_{(1,1)} \quad Z_{(1,1)} \right] & \cdots & \left[I_{(1,N)} \quad X_{(1,N)} \quad Y_{(1,N)} \quad Z_{(1,N)} \right] \\ \vdots & \vdots & \vdots \\ \left[I_{(M,1)} \quad X_{(M,1)} \quad Y_{(M,1)} \quad Z_{(M,1)} \right] & \cdots & \left[I_{(M,N)} \quad X_{(M,N)} \quad Y_{(M,N)} \quad Z_{(M,N)} \right] \end{array} \right\}$$

4.5.3 Result of Data Simplification

The work of original PCD simplification is deployed through MATLAB. As mentioned in section 4.2, the correct PCD data format for the software to return expected structure is in ASCII format. After the data is simplified, density of the original extracted data is decreased from 97,668 points to 14,000 points. This density decrease corresponds to the spacing of the printer head nozzles, so that, the distance between each two adjacent points along x-y plane is 1/96 inch (0.264 mm). The result of the simplified data is sampled and aligned equally in x and y direction (see figure 4.16).
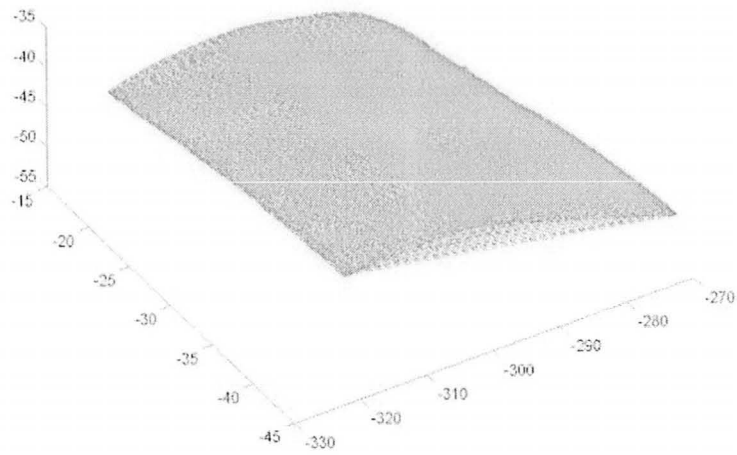
a) Extracted Original PCD
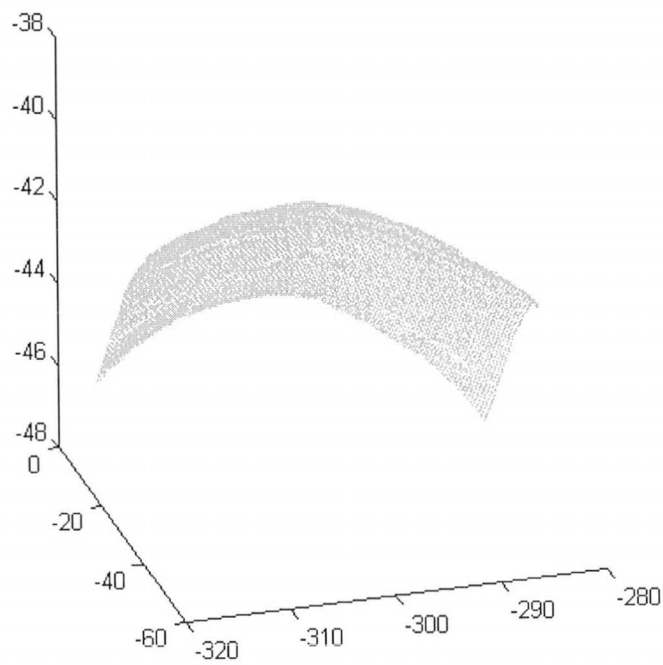
b) Simplified PCD of Image area

Figure 4.16 Result of PCD Simplification (All Units in mm)

4.5.4 2-D Image Construction

Grayscale Image

The simplified *Ps* matrix returns a $M \times N$ cell array. Each cell contains information of one point. Average intensity values have been calculated as $I_{(m,n)}$. A grayscale image can be constructed by mapping the intensity information on new image bitmap structure. Each intensity value is extracted and deposited to a new 2D bitmap according to its position in the cell array. The mathematical model for the gray scale bitmap matrix is shown as the following:

$$
I_{gray} = \begin{bmatrix}
I_{(1,1)} & I_{(1,2)} & \cdots & I_{(1,N)} \\
I_{(2,1)} & I_{(2,2)} & \cdots & I_{(2,N)} \\
\vdots & \vdots & \vdots & \vdots \\
I_{(M,1)} & I_{(M,2)} & \cdots & I_{(M,N)}
\end{bmatrix}
$$

Since the intensity collection range of the laser digitizer system is set as [0, 380,000], we can create standard double array gray scale image I_{gray} with a standard gray range of [0, 1] by dividing the image matrix by 380,000.

The gray image result that has been plotted in figure 4.17 also shows the quality of the digitized image. The image digitization and extraction are successful that the visualization extends to the cracks of the pre-coat on the surface. The exact size for this x-y plane-projected image can be calculated as 26.4mm× 36.96mm, from adjacent pixels distances of 0.264mm (1/96 inch).

Figure 4.17 Result 2-D Gray Scale Image

Image Binarization

The grayscale bitmap image needs to be transformed to binary image due to the employed single color printing system. In the new binary image, instead of having intensity information for each pixel, only 1 and 0 construct new binary image array. The binary image that has been thresholded contains only two classes of pixels, background (white) and foreground (black).

Otsu's threshold algorithm [46] is used to perform binarization task. Otsu's method is a relatively easy image threshold method that it distinguishes the threshold level by creating and analyzing the histogram of pixels intensities of gray image. Then, it searches for the threshold that minimizes the intra-class variance [46]. However, it cannot perform a proper job if the image is badly illuminated and contains high level of shadows and noise. The reason of choosing Otsu's algorithm in this case is because the gray scale pattern has very clear image and good quality of contrast [47]. The nice contract condition guarantees negligibility of low level noise. It returns a result that no scanned surface condition traits, for example cracks and porosities, appear on the binarized image. MATLAB contains the Otsu's algorithm in its image processing tool box by employing the function code *im2bw* [45, 46]. The binary image result is displayed in figure 4.18.

Figure 4.18 Binary Image

Visualization of 3D Decoration Plotting

Visualization of the 3D decoration plotting can be achieved through MATLAB by creating a filter for constructed cell-array matrix P_s, so that only the geometry for foreground is plotted (see figure 4.19).
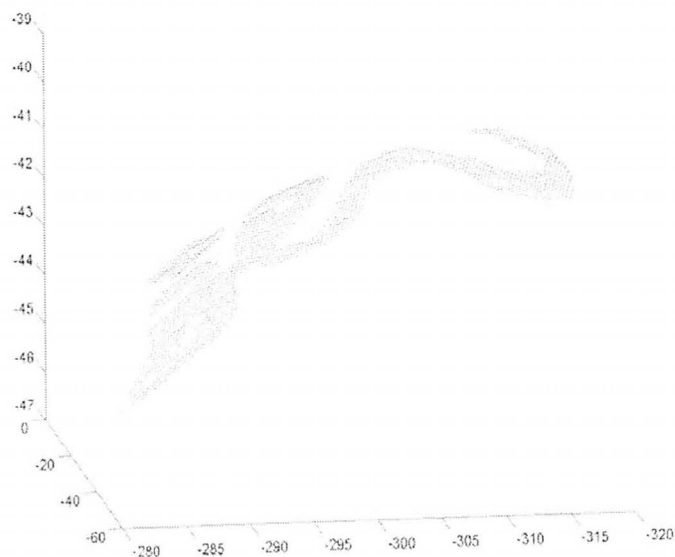

Figure 4.19 Visualization of 3-D Decoration Plot (All Units in mm)

4.6 Reproduction of Surface Decoration

Reproduction of hand-drawn surface decoration is implemented through the established oriented 3-D ink-jet printing system. Result of the re-engineered surface image shall achieve a certain level of accuracy, which can be only ensured by precise calculation of the print system orientation.

4.6.1 Printing Strategy - Ideal Projection of the Image

The constructed 2D bitmap is actually an image projection process that it perpendicularly stamps the decoration from B-Spline surface to x-y plane. Due to the specification of data simplification, the tolerance of the character edge is within + 0.264 mm along both x and y directions.

If the 2D image is projected back to the B-Spline surface, theoretically, this projected-back character feature locates at the same position of the surface as the original hand drawn pattern, which is described in figure 4.20. However, a certain sacrifice of resolution consistency is inevitable. The issue of this inconsistence can be negligible if projected surface normal has a slow rate changing through surface profile.

This projection method is ideal for the printing system because if the surface is too bumpy the printing job may not be appropriate due to the specification of restricted printing position to the product surface. The printer head cannot spray the ink accurately on the surface if the elevation of the print head deviates too much from optimum value. Also, the inconsistency of the resolution caused by great elevation changing along surface profile can cause bad quality for the printing result. Proper orientation of ink-jet printing system needs to be done through surface analysis and specific trajectory generation.
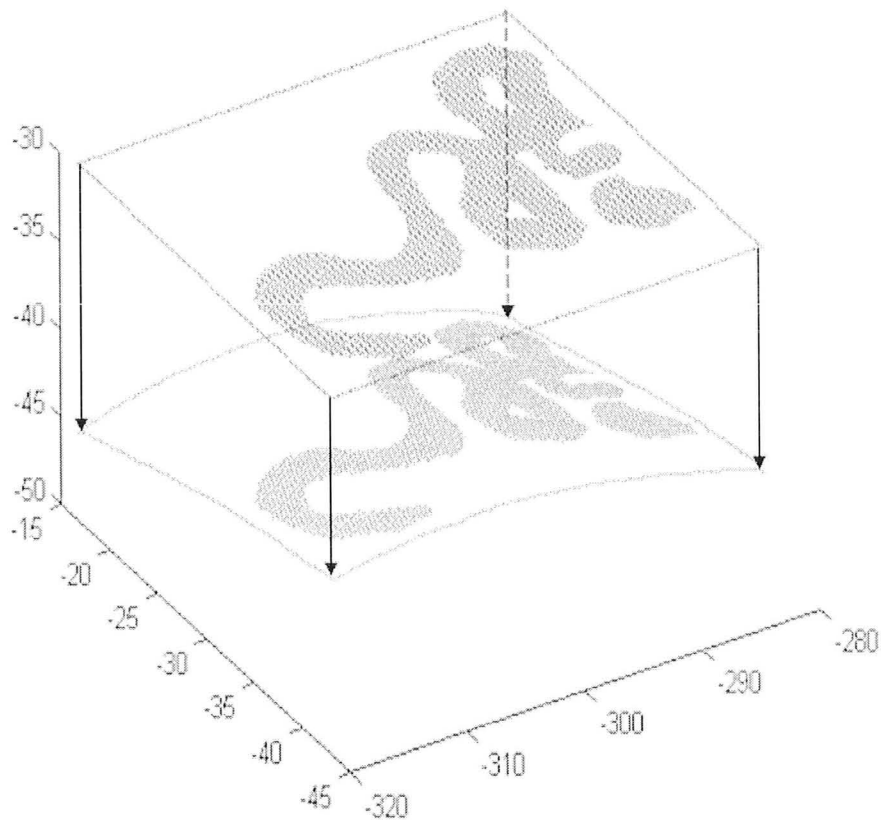
Figure 4.20 Ideal Projection from x-y Plane to B-Spline Surface (All Units in mm)

4.6.2 Establishment of Relevant Coordinate Systems

The oriented 3-D printing process for decoration reproduction requires establishment of relevant coordinate systems so that the original data of the image geometry matrix can be transform to local printing system. The given method that is used to apply for it is called 3-2-1iterative system alignments. The source code is provided as MATLAB program. 3-2-1iterative system alignments only require three points to create a coordinate system, so that x-y plane can be defined by all three points first. Then, two of the three points are used to locate its x axis. Finally, one of the two points is defined as local origin.

Local CMM Environment Setup

The CMM system automatically aligns its origin to a home position with specific x, y and z axis. To set up the first local coordinate system, an aluminum fixture plate, as figure 4.21 a) shown, are installed parallel above the CMM's granite foundation so that z-axis of universal coordinate system is consistent with the fixture normal. The standoffs, shown in figure 4.21 b), are used to guarantee repeatability of part setup for printing. They are screwed to the aluminum plate in order to constrain movement of the work piece. The fixture setup can ensure less than 30 μm error between the local fixture x-y and universal CMM x-y planes. This is verified by measuring each end of the fixture plane corners.
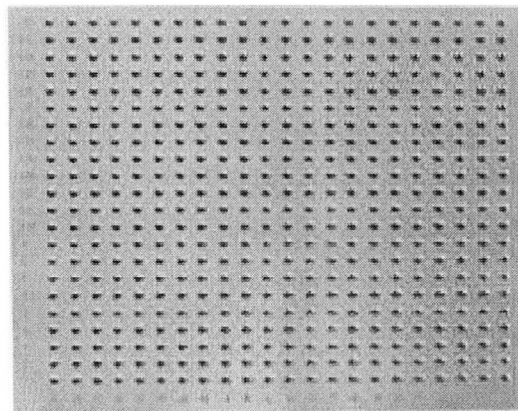
a) Aluminum Fixture Plane
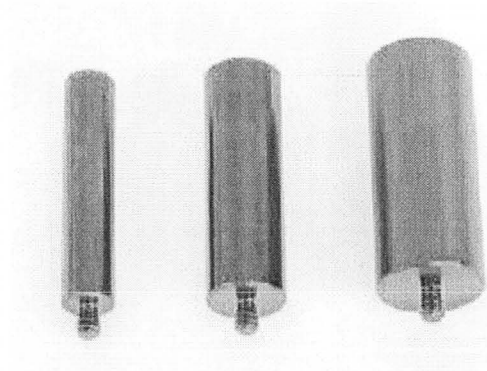
b) Standoffs

Figure 4.21 CMM Foundation Fixture

Establishment of Part Coordinate Systems

A specific jig for product part settlement is established as figure 4.22 described. Three unique standoffs are screwed precisely on a coated steel plane that two along the x-axis and one along the y − axis. As mentioned in section 4.4.1, the establishment of this jig corresponds to the datum plane that has been set for CAD model construction. All top surfaces of three standoffs have been pre-coated by InkAID white Matte [44] for geometry collection. The combination of the jig plane and the three standoffs restrict the six degrees of freedom for any properly placed object. Then, it is placed on aluminum fixture plane and locked by pre-assembled standoffs. By touch probe measurement for the cylindrical centers of three standoffs on pre-coated top surfaces, the coordinates of 3 points can be determined for 3-2-1 system alignment to establish a local part coordinate system.

The result of 3-2-1 coordinate system offers a standard 4 × 4 transformation matrix that can align universal machine coordinate system (MCS) to local part coordinate system (PCS). According to the rotation movements and translational information for the origin, if translational vector is $[x_{centertrans};\ y_{centertrans};\ Z_{centertrans}]$, the theoretical solution for the transformation matrix M_p can be expressed as following :

$$M_p = \begin{bmatrix} \cos(\theta) & -\sin(\theta) & 0 & x_{centertrans} \\ \sin(\theta) & \cos(\theta) & 0 & y_{centertrans} \\ 0 & 0 & 1 & z_{centertrans} \\ 0 & 0 & 0 & 1 \end{bmatrix}$$

In this project, θ is approximately equal to zero degree according to the foundation setup.
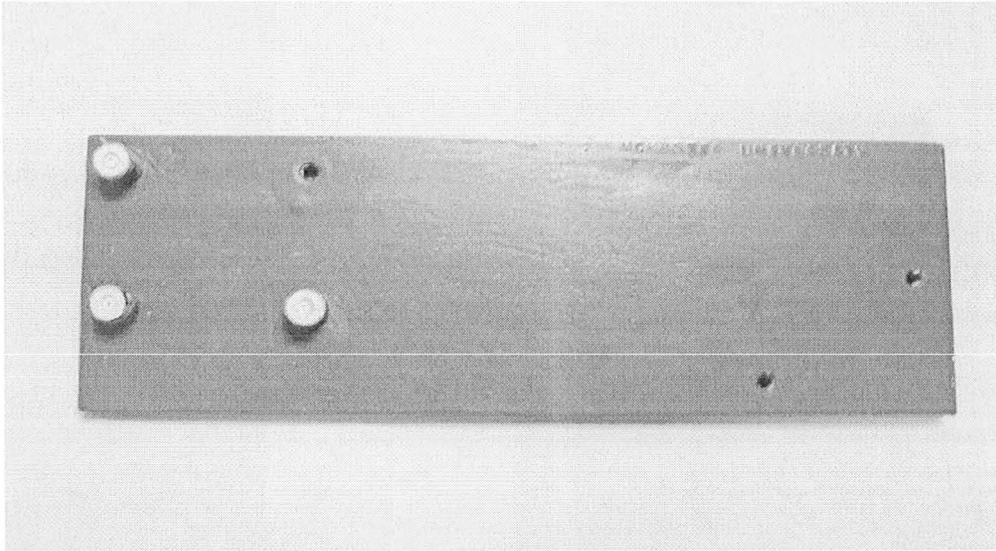
Figure 4.22 Part Jig to Place Product Part

In addition, the digital geometry data of the image also needs to be converted to the part coordinate system. Since the geometry of top surfaces for the three posts has been recorded by laser scan, they can be extracted and import to Imageware to locate the centers. In figure 4.23, three random picked points along circular edge allow the software to calculate the center of the top surface for cylinder. To ensure the accuracy, more center points are calculated to generate an average value for the center. Finally, the point could data conversion between MCS to PCS can be expressed using the following equations:

$$PCD_{MCS} = M_p \bullet PCD_{PCS}$$

and

$$PCD_{PCS} = M_p^{-1} \bullet PCD_{MCS}$$

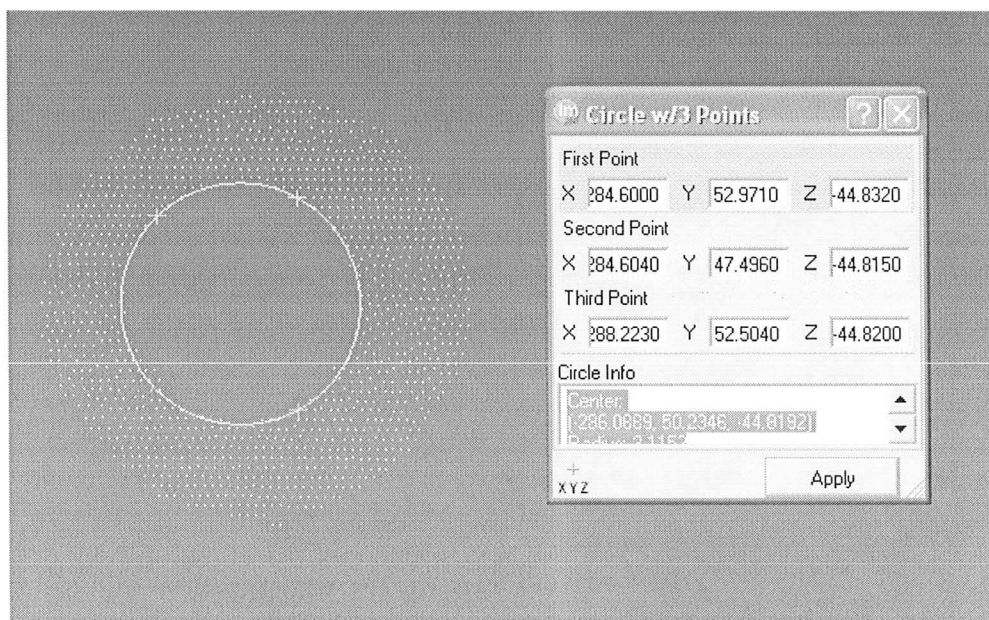Figure 4.23 Center Determination for Cylinders of Standoffs

4.6.3 General Surface Analysis

As it has been describe in section 4.2 and 4.3, the body Coons patch B-Spline surface of the object can be counted as 3 portions, and the middle portion 'A' (see figure 4.10 b)), where image locates, is relatively flat. If an artificial hull is constructed to cover the surface to facilitate the visualization analysis as figure 4.24 a) shown, it is apparent that the surface is approximately unique through two directions and can be regard as a standard inclined B-Spline extrusion. Two directions are named as U and V to approximate the uniformity of the surface.

The inclined B-Spline extrusion allows us to track the image along B-Spline trajectory through U direction. However, along V direction, the printing trajectory is approximately linear. The extraction of upper and left edges of the simplified image PCD is good enough for generating printing trajectories along U and V directions as figure 4.24 b) displayed.
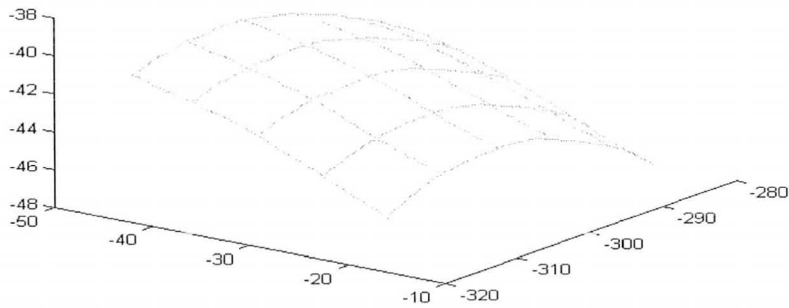
a) Hull Construction from Simplified PCD
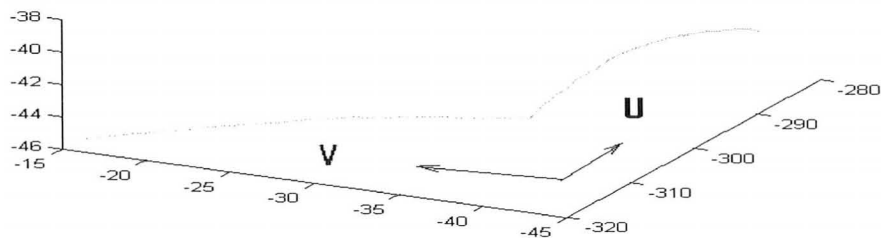
b) Two Directions of One Dimensional B-Spline Surface

Figure 4.24 Surface Analyses for Printing Trajectories (All Units in mm)

4.6.4 Generation of Printing Trajectory

Conclusion of the surface analyses shows the surface of image area is approximately uniform through 2 directions along the two edges. It is consistent with the capability of the Renishaw PH10M probe. Since the PH10 probe can rotate around two axes the combination of CMM movement and orientation of the probe will ensure a proper image printing process.

The extraction of the geometry for image edge along two directions can offer proper trajectories for printer. However, the trajectories of the printer also need to

meet the criteria of the printing specification. First of all, PH10 probe is limited for smallest angular increments of 7.5°, which allows rendering any theoretical curve path into connected section lines within the smallest angular increments. This can be achieved by tangent analysis along the extracted edges profile. Furthermore, since the optimal distance between HP printer head and product decorating surface is known as 1±0.5 mm, the sectioned lines can be compared to their corresponding surface profile to evaluate conformity for this tolerance.
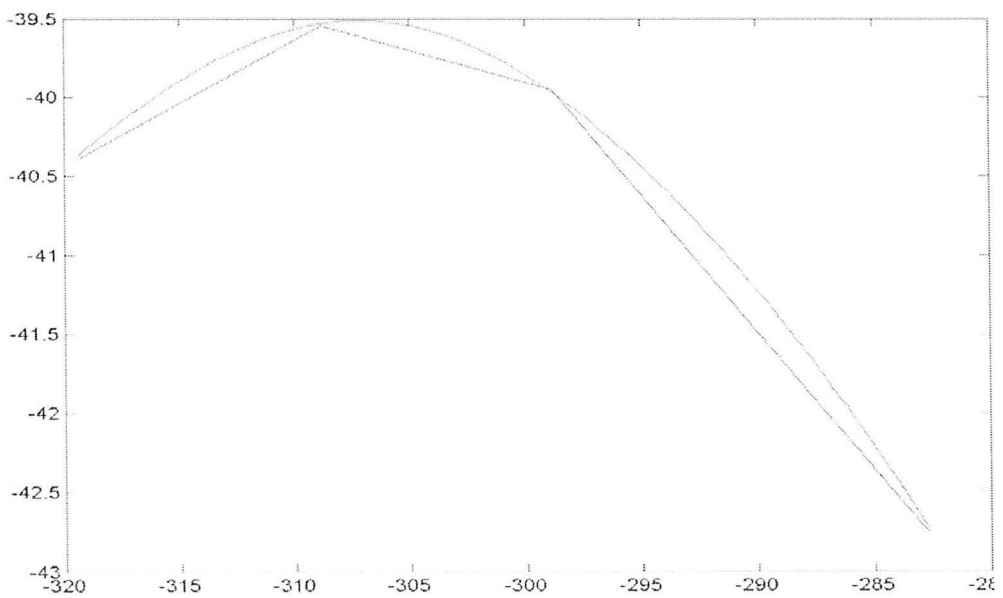
Trajectory for U Direction

Regarded as a B-Spline, the edge point cloud along U can be fitted to a real B-Spline curve through Uniform Parameterization Least Squares B-Spline fitting Algorithm in MATLAB. As it has been described in section 4.4.1 and section 2.5.1, the solution provides the sample points and control points to construct a better shaped B-Spline in associated CAD software. The residual error of this least squares B-Spline fitting algorithm can be controlled through changing number of sample points. In this project, the residual error has been decreased to less than 80 μm so that the residual effect to printing process can be totally ignored.

In order to extract the tangent values from B-Spline extrusion, the upper edge profile of the extrusion is isolated for investigation. A Visual Basic (VB) macro has been offered to utilize the 2D curvature evaluator in Inventor, where a function code is provided for extracting the tangent values along the B-Spline curve. This macro process is shown in figure 4.25 a).

By defining process width based on displayed x value, where the value represents the whole arc length along x-axis, the wrapped image length along this direction can be identified. The starting point bracket allows the input of the image starting point along x-axis, and it gives a line passing through the starting point and parallel to the y−axis. With the starting point and image wrapped range, the macro calculates an array of equidistant points, where they are located at a distance of 1/96 inches from each other along the B-Spline. For each point in the array, the corresponding tangent value is also calculated.
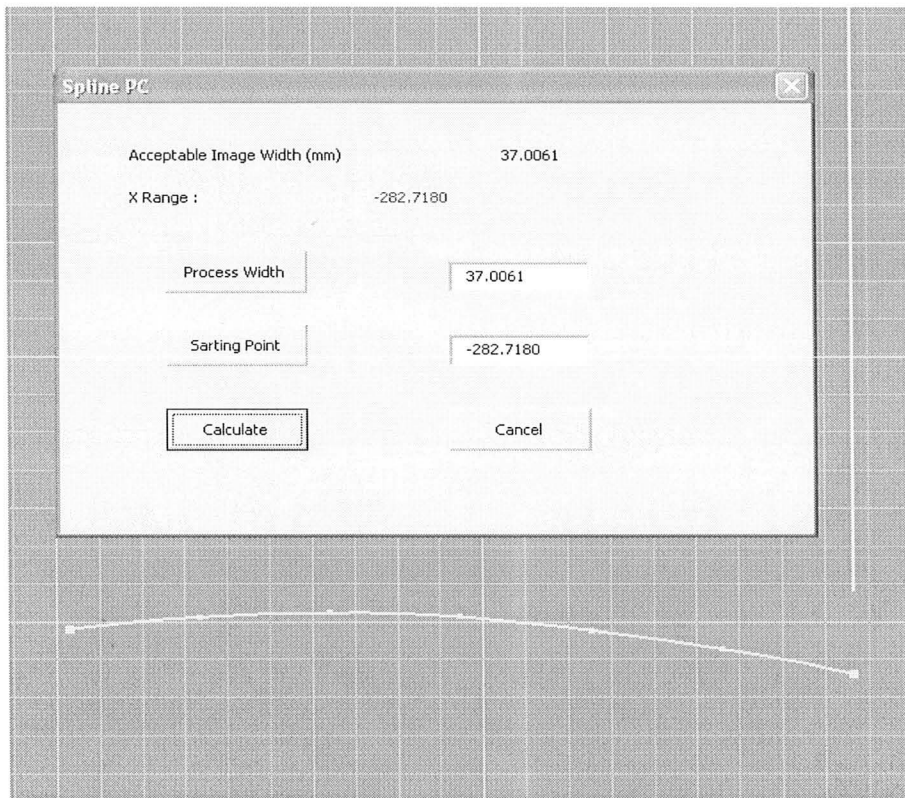
a) Generation of Normal for B-Spline by VBA Marco

b) Profile Curve V.S. 7.5° Line Sections

Figure 4.25 Trajectory Generation through U Direction (All Units in mm)

These values are stored in a text file as a structure of t × 3 matrix with the information as [x_t, y_t, tangent$_t$], where t represents the sequential number of the extracted array, so that it can be processed in MATLAB. In MATLAB, ranges of arc segments are described based on the tangent information, where the tangent variation within an arc segment is less than 7.5°. Section lines of all arc segments can be plotted to express the orientation condition for PH10 probe.

The result of B-Spline least squares fitting curve and its corresponding sectioned lines can be display in the same graph as figure 4.25 b). It is apparent that the elevation difference between section lines and their correspondent curve segments are all less that 0.3 mm along the normal of section lines. Comparison between the section lines and real curve draws a conclusion that if the PH10 probe is orientated according to the section lines the result must achieve requirement of optimal printing condition along U direction. Accordingly, the image can be sectioned with respect to the sectioned lines and orthogonally deposited to the surface from the start point of the determined B-Spline arc as figure 4.26 shown.

From figure 4.26, the printing orientation scenario for this project is to rotate the printer head three time along section line so that, within the range of one segment, the printing direction along 12 nozzles shall be fixed parallels to the section line. The calculated rotating angles for each corresponding section are 4.58°, -2.32° and -9.87°. The best orientation solution for the probe along U direction is 7.5°, 0° and -7.5° with respect to their segments. Obviously, the error is as small as 2~3 degrees.

However, according to specification of PH10 probe and equipment setup in chapter 2, only A-joint phase rotation is able to achieve the required movement. On the contrary, the rotatable range is [0°, 105°] with initial position of 0°. The problem of quadrant shifting can be solved by 180° rotation for probe head through B-joint phase as figure 4.27 shown.
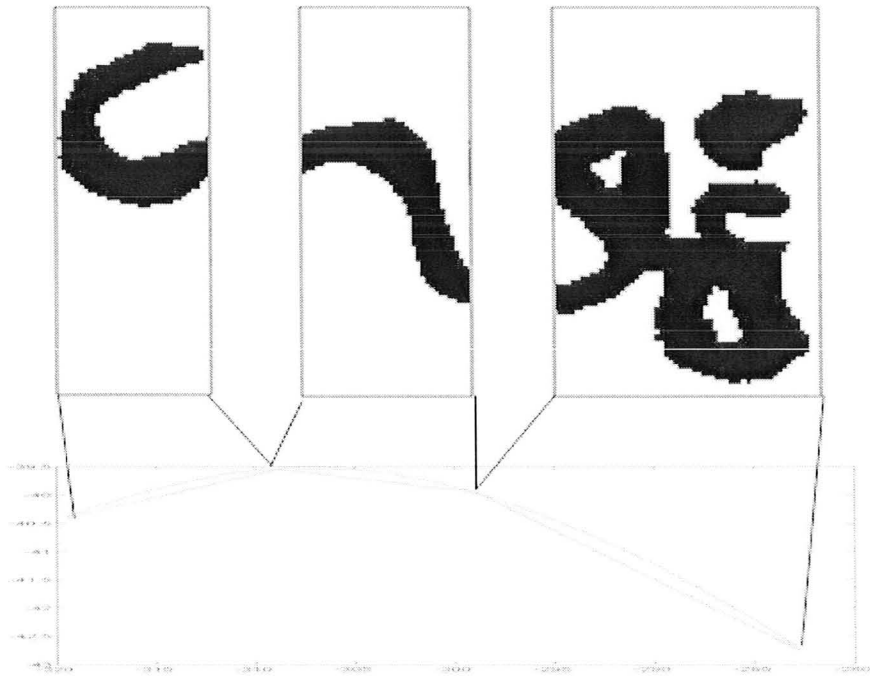
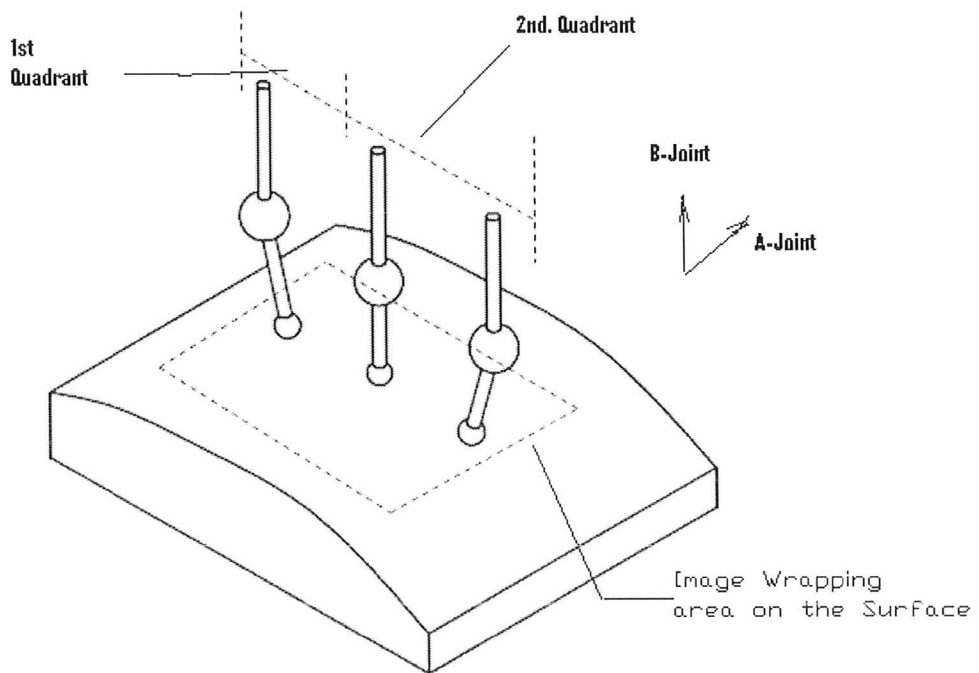Figure 4.26 Image Sectioning According to Arc Segments

Figure 4.27 System Orientation for Quadrant Shifting

There are two apparent shortages that come from this path generation. First, each step of the orientation through B joint requires system to perform one time of system alignment. Although it is automatic the time cost is inevitable. Secondly, along V direction it is not allowable for more probe orientation due to its limited functionality. The printer can never be aligned to be perpendicular to the surface along this direction. The only adjustment through V is to control the elevation by CMM to fit the optimal printing condition. However, causing by this adjustment, the risk of colliding between the printer head to the product surface may occur.

Trajectory for V Direction

According to the analysis for V direction edge, the B-Spline surface extrusion is mostly inclined along V. The confirmation of this linear fitting can be done by linear regression assessment. The result of linear regression approximation is plotted in figure 4.28 that the tangent of the inclination can be calculated. It is equal to 10.7° with 93 % of conformity. If probe orientation for A-joint phase can be applied along V direction with scarification of U direction the rotation angle shall be fixed to 7.5°. In this method, the image projection through ink-jet printer is inclined according to the calculated result of rotation angle and projected onto the object surface as figure 4.29 illustrated.
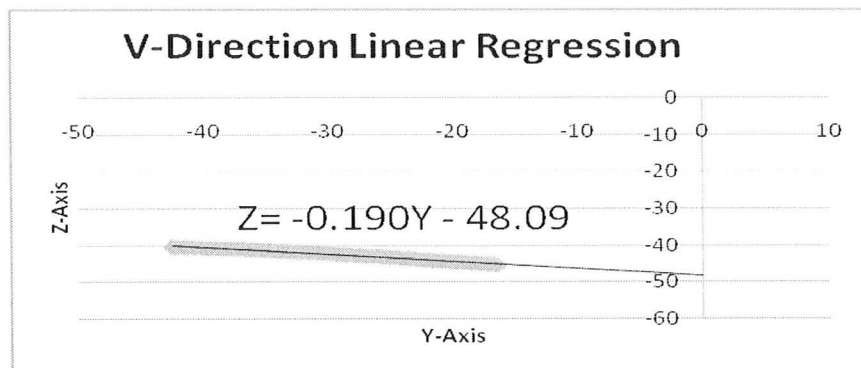

Figure 4.28 Linear Regression Assessment for V-Direction Printing Trajectory (All Units in mm)
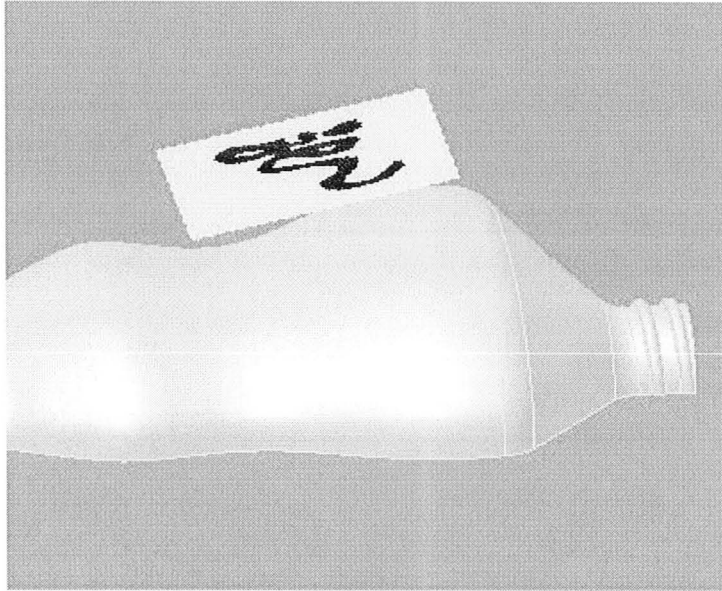
Figure 4.29 V-Trajectory Image Projection

Compensated Printing Trajectory

To compensate trajectories for U and V directions, investigation for each of their printing scenarios is deployed in chart 4.1. The result can be compared for decision making of a proper printing plan by referencing the optimal printing position. For the system orientation according to U trajectory, the deviation along the B-Spline profile is negligible. On the contrary, its maximum deviation between the printer and the product surface is approximately 8 mm along V direction. Since manipulating the printer head along z-axis can cause its collision to the product surface, it is impossible to improve the deviation with this U-direction trajectory setting. This is far exceeding the optimal printing position tolerance.

	MaxDeviation along U	MaxDeviation along V	Image Shrinkage	Resolution Inconsistence	Orientation Times
U Trajectory	Within optimal range	8 mm	Along U	Existing	Once
V Trajectory	3 mm	Within optimal range	Along V	Existing	Twice

Chart 4.1 Comparisons between Two Printing Trajectories

For the system orientation according to V trajectory, the maximum deviation occurs along the B-Spline profile as around 3 mm. Although it is out of optimal printing range, this is acceptable to perform a proper printing. A compensated printing trajectory is demonstrated from V trajectory that the orientation through A-joint angle is applied with its calculated inclination. In this situation, A-joint angle matches x-z plane of CMM coordinate. However, feeding of printer head has to be parallel to x-axis along U direction, and there is no probe orientation through B-joint angle.

For this compensated printing method, the printer only required one time orientation for initial V-direction inclination to perform decoration printing. This compensated printing trajectory must be chosen not only because of much higher printing efficiency but also because of its applicability.

This compensated printing method is a V-direction inclined projection. Theoretically, image deficit can be demonstrated as resolution inconsistence along profile direction (U) and uniform image shrinkage through inclination direction (V). The project-back printing method insures that there is no image profile dislocation along U direction. The resolution inconsistency, thus, is inevitable due to the curvature along U. By inclining the printer through V, it gives a shrinkage result for the image due to inclination projection. The total shrinkage along V can be calculated as 0.25 mm. Both of these image deficits are too small to be sensed by eye.

Printing Movement

According to the compensated printing trajectory displayed in figure 4.29, a typical inclined planar print [3] is applied. Figure 4.30 describes the actual printing process with orientation situation for employed oriented 3-D printing system. If let β equal to the surface inclination (7.5° for this case), after the probe is orientated to angle β, each incremental step of the CMM feeding can be defined as the following equations with introducing the printing resolution of 1/96 inch:

$$x_{increment} = \frac{\cos\beta}{8} \quad inch$$

$$y_{increment} = \frac{1}{96} \quad inch$$

and

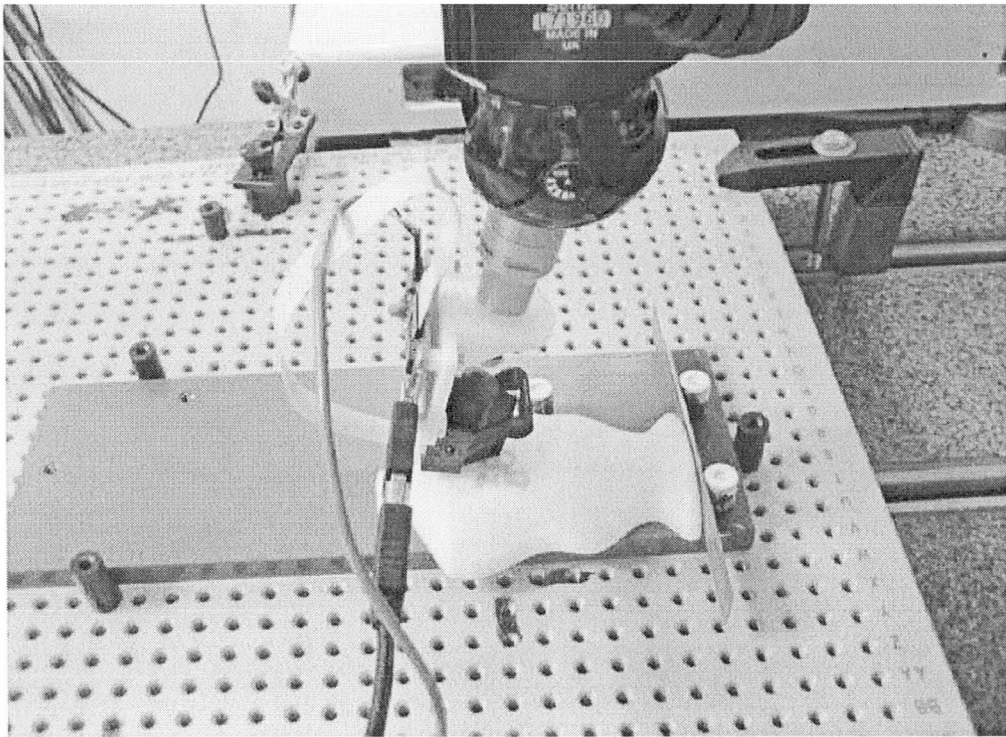$$z_{increment} = \frac{\sin \beta}{8} \quad inch$$

Figure 4.30 Compensated Printing Status

4.6.5 Calibration for System Accuracy

Before any printing work the system needs to be calibrated to diminish the error caused by mounting of the printer head. In order to mount the printer head on to the Renishaw adapter, a rapid prototyped mount component was designed and produced. Inaccuracy occurs during installation process due to the surface flatness of mount component, as well as parallelism problem from screw threading. This so-called Abbe error [48] is amplified along axial displacement during system angular

rotation as figure 4.31 shows.

To solve the problem, we can determine the distances from the centre of rotation and the edges of the different angles. The difference can be viewed on the print out for different angular print through probe rotation angle B and angle A. To calculate along z-axis and y-axis, the Abbe error can be measured and calculated along x, y axis and x, z axis correspondently. Then, the error factor can be eliminated by adding it to the total x and y offsets or x and z offsets for system transformation.
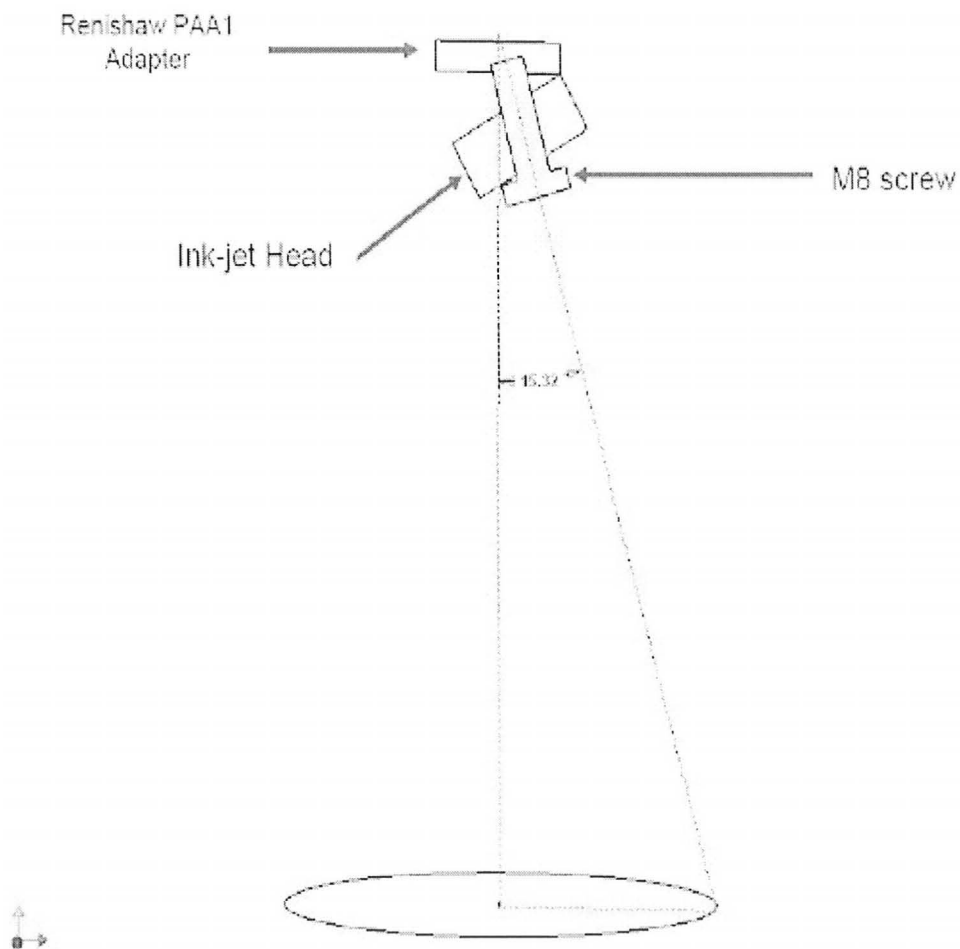

Figure 4.31 Extravagation of Abbe Error Fact [48]

Any combination of two-joint orientation of the PH10 probe requires two calibrations: the xy with the z− axis as the axis of rotation for probe phase B, and the

xz with the $y-$ axis as the axis of rotation for probe phase A. The calibration method was developed and deployed before this project by El Sahi [48].

Chapter 5

Results with Verification

In this chapter, project results from the workflow are displayed. Measurements are taken to verify the quality for decoration reproduction.

5.1 Results

By application of specified new product development workflow, all object models, including hand crafted clay model, digital CAD models and rapid prototype model are produced. All constructed models are listed in the following from figure 5.1 to 5.4. Decoration reengineering work is displayed clearly in figure 5.5. In figure 5.6, comparison between initial hand-made model and final rapid prototype product can be viewed. In general, the designed workflow successfully transfers the input of hand crafted clay object to the output of rapid prototype product with reproduction of surface decoration.
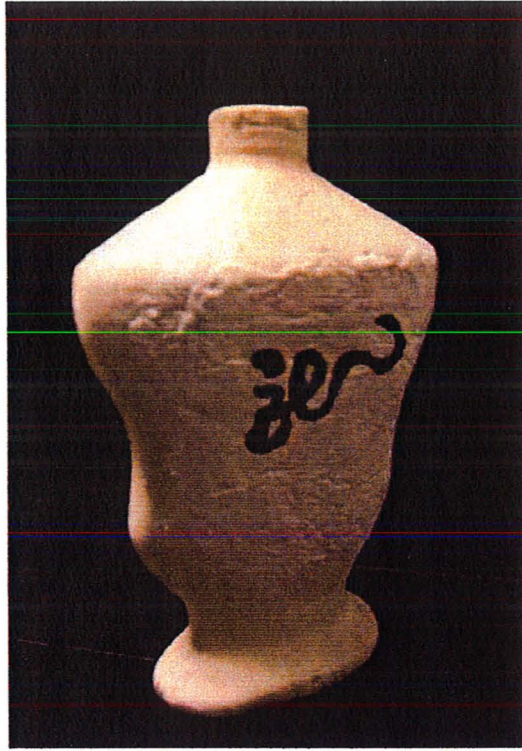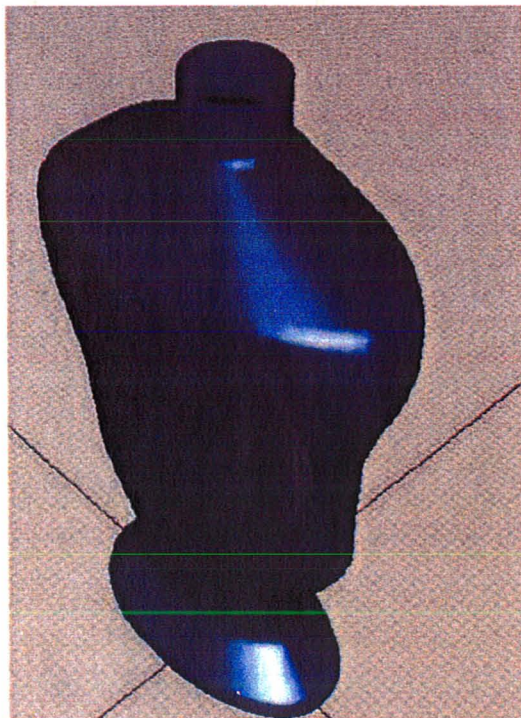
Figure 5.1 Product Hand Crafted Model

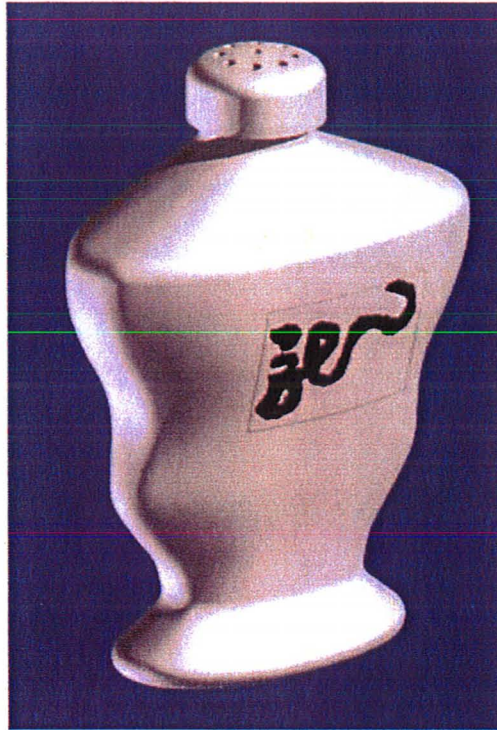Figure 5.2 Product Conceptual CAD Model

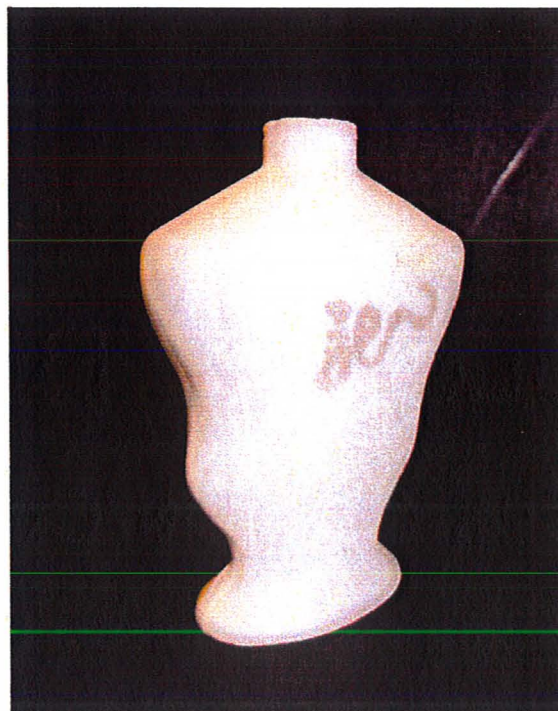Figure 5.3 Detailed CAD Model with Decoration

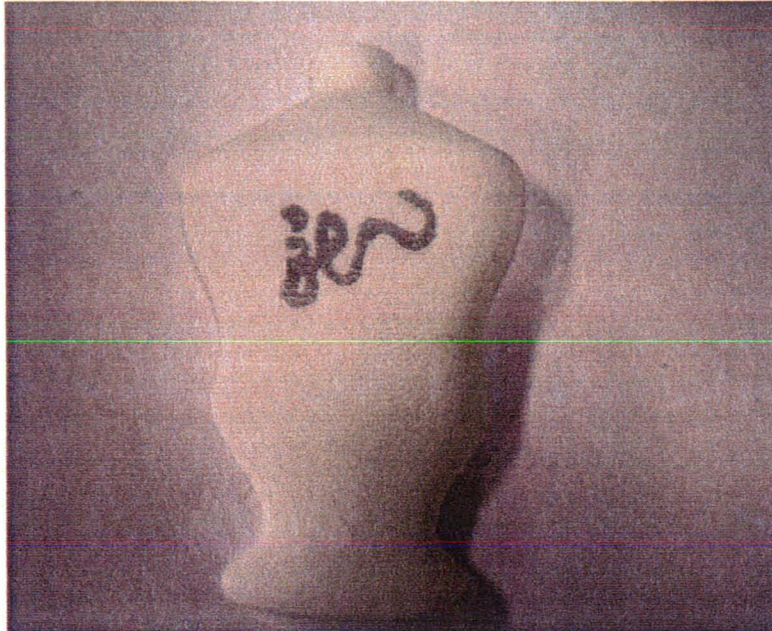Figure 5.4 Rapid Prototype Model with Decoration Reproduced

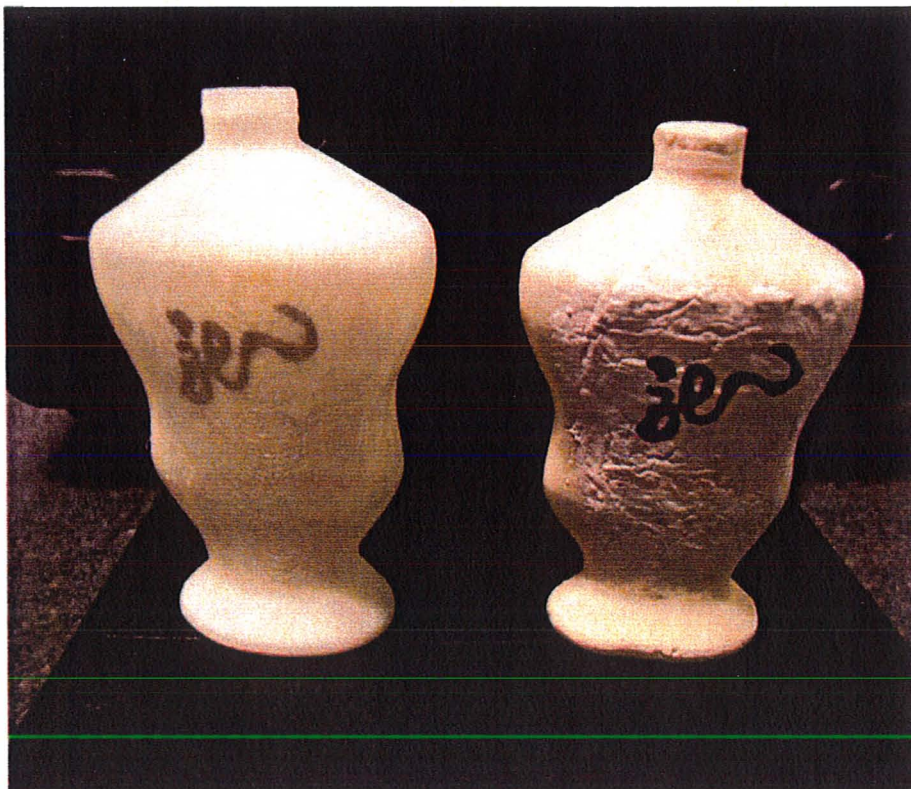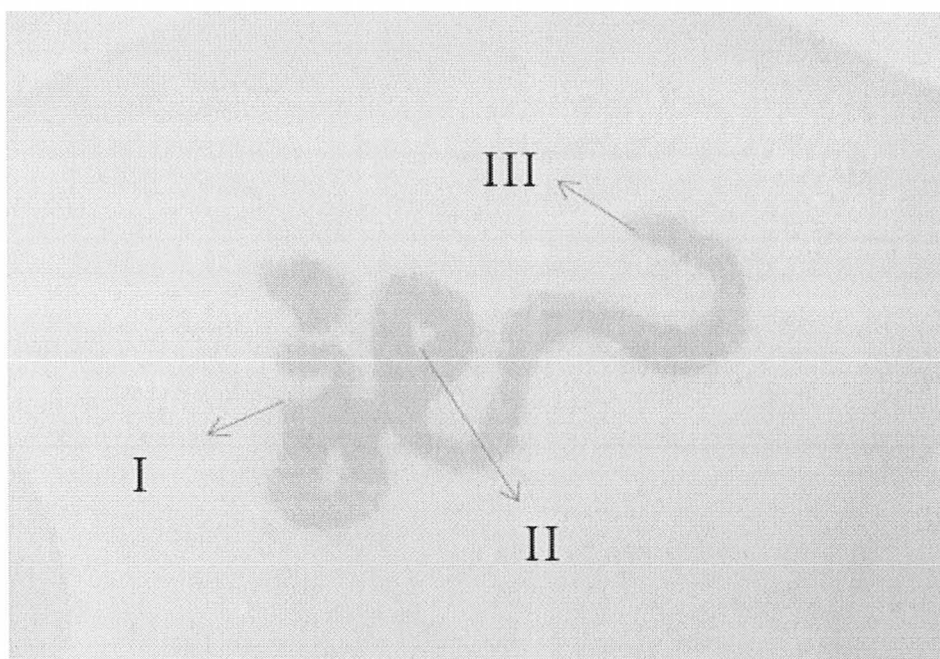Figure 5.5 Result of Decoration Reproduction on RP

Figure 5.6 Comparison between Workflow Input and Output
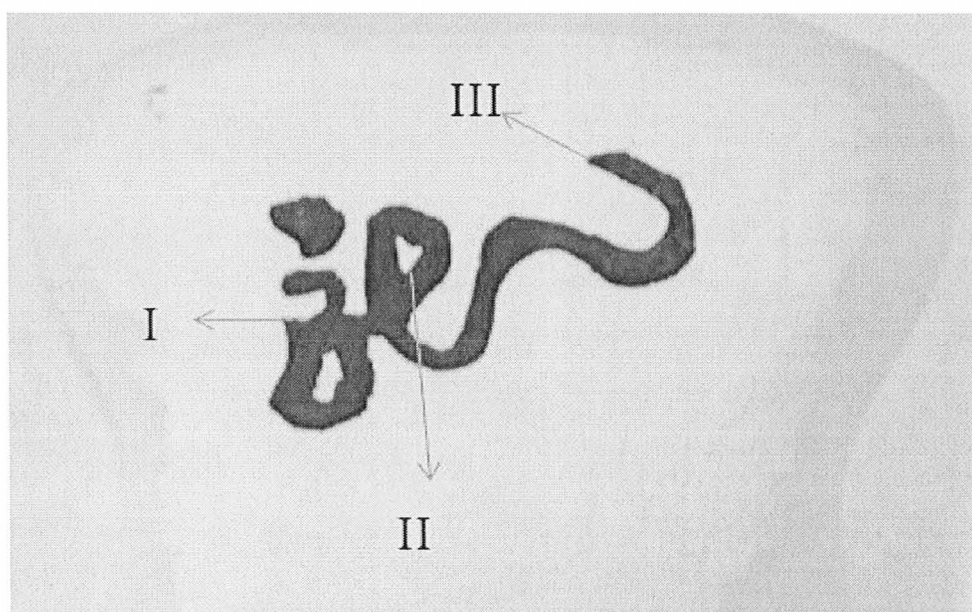
5.2 Verification for Reproduced Decoration

In order to verify that the location of reproduced decoration on rapid prototype is the same as where the hand-drawn pattern locates on clay model, a measuring process is deployed. First of all, the HP 56104 printer head is replaced by regular touch probe to re-establish CMM measuring functionality. Without any movements of the established fixture part jig in the CMM environment, hand crafted prototype and reproduced rapid prototype are individually and sequentially placed on the part jig to take measurements. Then, the several significant points on decorated image are chosen to be measured by CMM touch probe.

Displayed in figure 5.7, there are three points on the surface pattern that picked to verify the decoration position. From the result, the maximum error along x, y and z axis for the three points between two product models is approximately 2mm. The average error is less than 1 mm. The implied repeatability distribution includes the significant factor of measurement variation, which is caused by visually aligning the touch probe to significant points on surface pattern.

The result satisfies the customer requirement because of the small uncertainty of repeatability and visual un-sensibility of decoration dislocation and deformation to original handcraft model. The verification provides the evidence to prove success of both reproductions of RP model from digital model, and decoration oriented by 3-D printing system.

a) Measured Points on Final Product

b) Measured Points on Handcraft Decoration

Figure 5.7 Geometry Verification for Decoration Reproduction

Chapter 6
Conclusion

A new product development workflow was introduced in the thesis to transform the art concepts to real product, which including the realization of decoration pattern. The workflow successfully converted a sample product (peppershaker) from input of art clay model to rapid prototype model with surface decoration. To obtain the final product, two custom built systems associated with CMM Machines were applied to achieve the tasks of art model laser digitizing, and final product oriented 3-D ink-jet decoration.

During the procedures of the workflow, a standard CAD product model was constructed from digitized point cloud date for rapid prototyping. Decoration information was extracted from original point could data to re-form an image for printing. Image processing successfully reduced the image resolution from original laser digitized grayscale intensity to suitable binary status for proper reproduction on the surface of rapid prototype model. The issue of addressing printing method for B-Spline extrusion by oriented 3-D ink-jet printing system was also solved.

Objective accomplishment by the introduced workflow implementation could be viewed through product results from each workflow process with verification of accurate reproduction of surface decoration.

A more practical implementation could use less expensive XYZ linear stages and small DC servo or stepper motors. An additional two rotary axes could be implemented to replace the Renishaw probe head, overcoming the current 7.5 degree step resolution. The remaining workflow would not be affected.

Reference

[1] G. F. Smith. *Quality Problem Solving.* ASQ Quality Press, Milwaukee, USA, 1998.

[2] C.K. Chua; R.K.L. Gay; S.K.F. Cheong and H.B. Lee. *Art-to-part Case Studies.* Computing & Control Engineering Journal, v 5, n 6, p 285-91, Dec. 1994

[3] S. El Sahi, Y. Jiang, and A.D. Spence. *Oriented 3-d Inkjet Print.* Computer-Aided Design and Applications, 3(1-4):399–406, 2009.

[4] 3D Art To Part.: San Rafael, CA, USA. http:// www.3darttopart.com

[5] S.B.Tang and D.W. Tu. *Theoretical Analyses of Laser Triangulation Range Imaging System Based on Synchronized Scanners.* Journal of Optoelectronics Laser, v 12, n 6, p 587-591, June 2001

[6] Arius3D Inc., Hymarc 3D Vision System: Nepean, ON, Canada. http://www.arius3d.com

[7] Arius3D Inc., *Hyscan 3-D Laser Digitizing System- Operator's Manual.* Nepean, ON, Canada. Currently available from: www.arius3d.com.

[8] Inition Inc.: London, UK. http://www.inition.co.uk

[9] Creaform Inc.: Levis, Quebec, Canada. http://www.creaform3d.com.

[10] FARO Technology Inc.: Beringen, Switzerland. http://www.faro.com

[11] Metris Inc.: Leuven, Belgium. http://www.metris.com

[12] D.G. Lamb; D.L. Baird and M.A. Greenspan. *An Automation System for Industrial 3-D Laser Digitizing*. Second International Conference on 3-D Digital Imaging and Modeling (Cat. No.PR00062), p 148-57, 1999

[13] Berntsen International Inc. *2004 3D Laser Scanner Hardware Survey*. Madison, WI, USA.
Available from: http://www.pobonline.com/POB/Protected/Files/PDF/0104survey.

[14] F. Blais; J. Taylor; L. Cournoyer; M. Picard; L. Borgeat; L.G. Dicaire; M. Rioux; J.A. Beraldin; G. Godin; C. Lahnanier and G. Aitken. *High Resolution Imaging at 50μm Using a Portable XYZ-RGB Color Laser Scanner*. National Research Council Canada, Ottawa, Canada, May, 2005. NRC 48099. Available from: http://nparc.cisti-icist.nrc-cnrc.gc.ca/npsi/ctrl?action=rtdoc&an=5765101&article=5.

[15] H.-L. Chan; A.D. Spence and M.P. Sklad. *Laser Digitizer Based Sheet Metal Strain and Surface Analysis*. Int. J. Mach. Tools Manufacture, 47(1), pp. 191-203, Jan. 2007.

[16] Direct Dimension Inc.: Owings Mills, MD, USA. http://www.directdimensions.com.

[17] S.O. Onuh and Y.Y. Yusuf. *Rapid prototyping technology: Applications and benefits for rapid product development*. Journal of Intelligent Manufacturing, 10(3):301 – 311, 1999. Available from: http://dx.doi.org/10.1023/A: 1008956126775.

[18] C.K. Chua; K.F. Leong and C.S. Lim. *Rapid Prototyping: Principles and Applications (2nd Edition)*. World Scientific Publishing Company, New Jersey, USA, Mar. 2003.

[19] J.P. Jarosz and I.J. Busch-Vishniac. *A topical analysis of mechanical engineering curricula*. Journal of Engineering Education, 95(3):241 – 242, 2006.

[20] Wikipedia. Stereolithography.
Available from: http://en.wikipedia.org/wiki/Stereolithography.

[21] Castle Island Co. *Rapid Prototyping and Solid Freeform Fabrication - The Worldwide Guide.* Available from: http://home.att.net/~castleisland.

[22] Stratasys, Inc. Eden Prairie, MN, USA. http://www.dimensionprinting.com.

[23] N. Hopkinson; R.J.M Hague and P.M Dickens, editor. *Rapid Manufacturing: An Industrial Revolution for the Digital Age.* Wiley, Chichester, West Sussex, England, 2006.

[24] Keith Hillestad. *Decorating methods and processes.* Flexography; Pad Transfer Printing. Rochester, NY, USA, 1996.

[25] R. A. Janco. Graphics for decorating plastics: Comparison of the four most common decoration methods. pages 1136 – 1138, Los Angeles, CA, USA, 1987.

[26] Electric Data Systems Corporation: Imageware 11, Plano, TX, USA. http://www.eds.com.

[27] Autodesk, Inc.: AliasStudio, San Rafael, CA, USA. http:// www.autodesk.com.

[28] Autodesk, Inc.: Inventor, San Rafael, CA, USA. http:// www.autodesk.com.

[29] Ibrahim Zeid. *Mastering CAD/CAM.* McGraw-Hill, New York, 2004.

[30] Kunwoo Lee. *Principles of CAD/CAM/CAE Systems.* Addison-Wesley Longman Publishing Co., Inc., Boston, MA, USA, 1999.

[31] PolyU Industrial Centre. Rapid Product Development Resource Centre. Available from: http://rpdrc.ic.polyu.edu.hk/content/rp_for_arch_short_guide.htm.

[32] Les Piegl and Wayne Tiller. *The NURBS book (2nd ed.)*. Springer-Verlag New York, Inc., New York, NY, USA, 1997.

[33] David Eberly. *Least-Squares Fitting of Data with B-Spline Curves*. Geometric Tools, LLC, Feb. 2008. Available From: http://www.geometrictools.com/Documentation/BSplineLeastSquaresFit.pdf

[34] J. C. Nash. *The Singular-Value Decomposition and Its Use to Solve Least-Squares Problems*. Compact Numerical Methods for Computers: Linear Algebra and Function Minimisation, 2nd ed. pp. 30-48, 1990.

[35] DEA Hexagon Metrology. North Kingstown, RI, USA. http://www.hexagonmetrology.us/dea.

[36] Renishaw. *PH10 Motorised Probe Head Series User's Guide, April 2006*. Available from: www.renishaw.com/media/pdf/en/7937578e157344a3b0f416f9cebd7a5c.pdf

[37] Hp TIG 1.0 print cartridges. Technical Report 5981-6812EN, Hewlett-Packard Development Company, L.P., West Bernardo Drive, San Diego, CA 92127, USA., Nov 2004. Available from: www.hp.com/oeminkjet/reports/TIJ1.0.pdf.

[38] Hp 51604 (51604a) refills. Available from: http://inkjetrefillkit.net/inkjetcartridge.php?cartridge=hp-51604&lazySID=vrqlTGTirEkuHTZHBlofFvfXy1216532147.

[39] Matt Gilliland. *Inkjet Applications with BASIC Stamp 2 and SX Microcontrollers*. Woodglen Press, 2005.

[40] Parallax INC. *96 dpi Serial Inkjet Printer Development Kit* (1.1 edition), Nov. 2005. Available from: www.parallax.com/Portals/0/Downloads/docs/prod/robo/InkjetKitDocs-v1.0.pdf.

[41] QNX Software Systems Inc.: Kanata, ON, Canada. www.qnx.com.

[42] J.O. Harris and A.D. Spence. *Geometric and Quasi-Static Thermal Error Compensation for a Laser Digitizer Equipped Coordinate Measuring Machine*, Int. J. Mach. Tools Manufacture, 44(1), pp. 65-77, 2004.

[43] Crayola: Lindsay, ON, Canada. http://www.crayola.com.

[44] Ontario Specialty Coatings Corp.: inkAID, Watertown, NY, USA. http://www.inkaid1.com.

[45] The Mathworks, Inc.: MATLAB® 6.5, Natick, MA, USA. http://www.mathworks.com.

[46] N. Otsu. *A threshold selection method from gray-level histograms*. IEEE Transactions on Systems, Man and Cybernetics, 9(1):62–66, January 1979.

[47] P.K Sahoo; S. Soltani; A.K.C. Wong and Y.C. Chen. *A Survey of Thresholding Techniques*. Comput. Vision Graphics & Image Process., Vol. 41, pp.233-260, 1988.

[48] S. El-Sahi. *Oriented 3-D Printing*. M.A.Sc. thesis, McMaster University, Dec. 2008.